1971

A study of the dislocation instability and reverse martensitic transformation in FE-NI system

Chung Lim

Department:

1. Iron-Nickel Alloy
I Title

A STUDY OF THE DISLOCATION INSTABILITY AND REVERSE MARTENSITIC TRANSFORMATION IN FE-NI SYSTEM

BY

CHUNG LIM, 1942-

A THESIS

Presented to the Faculty of the Graduate School of the

UNIVERSITY OF MISSOURI-ROLLA

In Partial Fulfillment of the Requirement for the Degree

MASTER OF SCIENCE IN METALLURGICAL ENGINEERING

1971

Approved by

(Advisor

ABSTRACT

Since the martensitic reaction is a strain transformation, the transformation of the lattice structure can be induced by an external stresses. This also means that the macroscopic total elastic constant should decrease as the temperature is lowered to M_s on cooling. For the reverse transformation an anomalous decrease of the elastic constant is to be expected as the temperature increases to A_s on heating.

In this experiment measurements of the velocity change of an ultrasonic wave in Fe-Ni alloys were carried out for the reverse martensitic transformation. The deviation from the linear relationship of the velocity change as a function of temperature is identified to be due to dislocation motion. An analysis of the data in terms of a dislocation string model applied to a stacking fault suggests that this deviation reflects the onset of the dislocation instability.

ACKNOWLEDGEMENT

The author would like to express his sincere gratitude and appreciation to his advisor, Dr. Manfred Wuttig, for his generous advice and encouragement.

He also wishes to thank Dr. Tetsuro Suzuki. Dr. Suzuki's kind and earnest guidance relating to this thesis was essential for the completion of this work. Appreciation is also expressed to his fellow graduate students for their helps in many aspects. Most of the alloys were kindly prepared by Mr. Robert B. Crosby of the United States Bureau of Mines-Rolla.

Most sincerely the author expresses his gratitude to his wife, Moon-Hee Lim, for her quiet and tender support.

TABLE OF CONTENTS

Page

ABSTRACT.....ii

ACKNOWLEDGEMENT.....iii

LIST OF ILLUSTRATIONS.....v

I. INTRODUCTION.....1

II. REVIEW OF LITERATURE.....3

A. STACKING FAULT WIDTH AND DISLOCATION INSTABILITY.....3

B. VIBRATING DISLOCATION MODEL AND THE STACKING FAULT WIDTH.....5

C. OBSERVATION OF THE VELOCITY CHANGE OF THE ULTRASONIC WAVE.....9

III. EXPERIMENTAL PROCEDURE.....14

A. ULTRASONIC MEASUREMENT.....14

B. THERMAL DILATATION MEASUREMENT.....22

C. SAMPLE PREPARATION.....22

IV. RESULTS AND DISCUSSIONS.....24

V. CONCLUSIONS.....43

VI. REFERENCES.....44

VII. VITA.....47

APPENDIX I - EQUATION OF MOTION FOR THE VIBRATING DISLOCATION MODEL.....48

APPENDIX II - ATTENUATION AND VELOCITY CHANGE OF ULTRASONIC WAVE.....52

LIST OF ILLUSTRATIONS

Figures Page

1. Temperature Dependence of ω_o^2 and $(\Delta V/V)_{dis}$ (schematic).....12

2. Prediction of $\Delta f/f$ vs. Temperature (schematic).....13

3. Schematic Diagram of the Ultrasonic Measurement.....17

4. Typical Pulse Echo Pattern (without specimen).....18

5. Pulse Echo Pattern with Adjusted PRT (without specimen).....19

6. Typical Pulse Echo Pattern (with specimen).....20

7. A Maximum Echo Amplitude when $PRT=2\Delta T$.....21

8. Relative Change of PRF for Fe-28.09%Ni Specimen.....29

9. Relative Change of PRF for Fe-28.34%Ni Specimen.....30

10. Relative Change of PRF for Fe-31.09%Ni Specimen.....31

11. Relative Change of PRF for Fe-31.95%Ni Specimen.....32

12. Relative Change of PRF for Fe-33.62%Ni Specimen.....33

13. Relative Length Change of Fe-28.09%Ni Specimen.....34

14. Relative Length Change of Fe-28.34%Ni Specimen.....35

15. Relative Length Change of Fe-31.09%Ni Specimen.....36

16. Relative Length Change of Fe-31.95%Ni Specimen.....37

17. Relative Length Change of Fe-33.62%Ni Specimen.....38

18. Relative Velocity Change of the Ultrasonic Wave for Fe-28.09%Ni Specimen.....39

19. Relative Velocity Change of the Ultrasonic Wave for Fe-28.34%Ni Specimen.....40

LIST OF ILLUSTRATIONS (continued)

Figures Page

20. Relative Velocity Change of the Ultrasonic Wave for Fe-31.09%Ni Specimen.....41

21. Relative Velocity Change of the Ultrasonic Wave for Fe-33.62%Ni Specimen.....42

I. INTRODUCTION

The martensitic transformation is commonly referred to as a diffusionless phase transformation which is observed in quenched metastable metals and alloys. Numerous studies [1-13] have been made on the crystallography and the kinetics of the martensitic transformation, but no understanding of the basic triggering mechanism of the martensitic transformation has been achieved yet. Studies on the parent phase just above the martensite-start temperature (M_s) on cooling and just below the temperature at which the reverse transformation begins (A_s) on heating are necessary.

Since the martensitic transformation involves shape deformations, the transformation of the lattice structure can be induced by external stresses at the temperatures above M_s. Scheil[14] showed that a slight increase of M_s occurs upon stressing a 29%Ni-Fe alloy. Other investigations carried out by Chang and Read[15] indicated an increase in M_s and a decrease in A_s in a Au-47.5%Cd alloy. According to Zener's interpretation, this means that the elastic modulus of the parent phase should decrease as the temperature is lowered toward M_s. This interpretation has not been supported firmly, mainly because of insufficient experimental data.

The purpose of this experiment is to extend the existing information and to apply the theory of the triggering mechanism[29,37] for the martensitic transformation and the

reverse transformation to the data obtained for Fe-Ni alloys.

II. REVIEW OF LITERATURE

A. STACKING FAULT WIDTH AND DISLOCATION INSTABILITY

According to Zener's interpretation of the martensitic transformation, the second derivative of the free energy of the parent phase becomes zero with respect to a certain shear deformation parameter X as the temperature is lowered to M_s (normal martensitic transformation):

$$\left(\frac{\partial^2 F}{\partial X^2}\right)_{T = M_s} = 0 \tag{1a}$$

An extension of this conjecture leads to an equivalent stability criterion for martensite on heating:

$$\left(\frac{\partial^2 F}{\partial X^2}\right)_{T = A_s} = 0 \tag{1b}$$

In other words, the parent phase becomes unstable at the M_s and A_s temperatures with respect to the thermal fluctuation of the parameter X. The physical nature of this parameter should then be examined in more detail.

If X means simply a macroscopic shear deformation parameter, $(\partial^2 F/\partial X^2)$ is equal to a linear combination of single crystal elastic constants. However, because the metal begins to transform before the total disintegration of the parent phase, the static elastic constants cannot be zero at the M_s and A_s temperatures. Consequently, the parameter X should represent a certain shear deformation other than a macroscopic total shear deformation.

It is well-known that the stacking fault is an embryo

for the transformation between H.C.P. and F.C.C. structures[17] and also between F.C.C. and B.C.C. (or B.C.T.) structures.[18,19] According to the dislocation model of the transformation,[6-12] the widening of the stacking fault can cause the triggering of the martensitic transformation. Therefore, it was proposed[29,37] that the unspecified parameter, X, will be associated with the widening of the stacking fault, i.e., with the antiparallel displacement of the partial dislocations bounding the stacking fault. The expression, $(\partial^2 F/\partial X^2) = 0$ at $T = M_s$ or $T = A_s$, then, means that the restoring force for the change of the stacking fault width becomes zero as the temperature approaches M_s or A_s.

The forces determining the stacking fault width are

1) line tension of the partial dislocations,
2) the surface tension due to the stacking fault energy, and
3) the repulsive interaction between the partial dislocations.

In a continum model, both the line tension and the repulsive force are given in terms of the shear elastic constant and Burgers vector of the dislocation. Since the elastic constants are montonic functions of temperature, the line tension and the repulsive force should have the same monotonic temperature dependence. Hence, the only possible source of the instability of the stacking fault width is the stacking fault free energy. The following approximations have been made[29,20] about the stacking fault

free energy, E, per unit area.

1) The absolute value of the stacking fault energy should decrease as the temperature approaches the phase boundary.
2) Stacking fault energy is positive for the high temperature phase and is negative for the low temperature phase.[20]
3) Stacking fault energy is expected to be dependent on the stacking fault width, 2X, as well as the temperature, T.

A simple expression satisfying above assumptions is given by[29]

$$E(T,X) = K(T-T_o) \pm a_2X^2 \pm a_4X^4 \pm - - - , \qquad (2)$$

where T_o is the temperature at which the stacking fault energy, E, becomes zero, and K, a_2, a_4, - - - are constants which do not depend on the temperature. The positive sign is valid for the martensitic transformation on cooling from the high temperature phase to the low temperature phase and the negative sign is valid for the reverse transformation on heating from the low temperature phase to the high temperature phase. The odd powers of X are absent because the stacking fault energy, E, is expected to be an even function of the stacking fault width, 2X.

B. VIBRATING DISLOCATION MODEL AND THE STACKING FAULT WIDTH

Wide attention has been given to the interaction between dislocations and alternating stress waves. It was

first suggested by Read[21,22] that the damping loss and modulus change observed in metals might arise from dislocation motion. Koehler[23] developed the idea that a dislocation line segment might vibrate in the presence of an alternating stress field and behave like a driven damped vibrating string. Nowick,[24] Weertman,[25] and Salkovitz[26] also proposed ideas for different damping models. The effect of crystal anistropy on the interaction of the dislocations with an applied stress wave as well as the effect on elastic constants was discussed by DeWitt and Koehler.[27]

Granato and Lücke[28] analysed the vibrating dislocation model by Koehler in more detail. The differential equation for that model is

$$A \frac{\partial^2 \xi}{\partial t^2} + B \frac{\partial \xi}{\partial t} - C \frac{\partial^2 \xi}{\partial y^2} = b\sigma, \tag{3}$$

where $A = \pi\rho b^2$ is the effective mass per unit length (ρ = density of the material, b = Burgers vector), B is damping coefficient per unit length, $C = 2Gb^2/\pi(1-\nu)$ is effective line tension (G = macroscopic elastic constant, ν = Poisson's ratio), σ is the induced stress, $b\sigma$ is the driving force per unit length of dislocation, y is coordinate along the dislocation line, and ξ is the displacement of the dislocation due to the stress applied.

For an analysis of martensitic triggering mechanism, Eq. (3) should be modified according to the assumptions described in section A. The modified equation of motion[29] of the half dislocation is

$$A \frac{\partial^2 X}{\partial t^2} + B \frac{\partial X}{\partial t} + C \frac{\pi^2}{l_o^2} X - C \frac{6\pi^2}{l_o^4} X^3 + - - -$$

$$+ K(T - T_o) \pm a_2 X^2 \pm a_4 X^4 \pm - - - = b\sigma, \qquad (4)$$

where A, B, and C are the same as in Eq. (3), l_o is the distance between the pinning points, the series of odd powers of X represents the contribution of the line tension (see Appendix I), and the terms $K(T - T_o) \pm a_2 X^2 \pm a_4 X^4 \pm - -$ represent the contribution of the stacking faults. The repulsive interaction between the partial dislocations is neglected here since it does not affect the qualitative analysis.

The stacking fault width 2X consists of a static part, X_o, and the time dependent vibrating part, ΔX, i.e.,

$$X = X_o + \Delta X . \qquad (5)$$

Assuming that the external stress contains no static components, we have

$$C \frac{\pi^2}{l_o^2} X_o - C \frac{6\pi^2}{l_o^4} X_o^3 + - - - + K(T - T_o) \pm a_2 X_o^2 \pm$$

$$- - - = 0. \qquad (6)$$

Solving Eq. (6) by sucessive substitution method (Iteration Method), we obtain approximate value of X_o given by

$$X_o = - \frac{l_o^2}{c\pi^2} \left[K(T - T_o) \pm a_2 \frac{l_o^4}{c^2 \pi^4} K^2 (T - T_o)^2 \pm - - - \right]. \qquad (7)$$

The equation of motion for the time dependent vibrational part, ΔX, can be obtained from Eq. (4), assuming Eq. (7) is a solution of Eq. (6),

$$A \frac{\partial^2(\Delta X)}{\partial t^2} + B \frac{\partial(\Delta X)}{\partial t} + C \frac{\pi^2}{l_o^2} X_o + C \frac{\pi^2}{l_o^2} \Delta X + - - -$$

$$+ K(T - T_o) \pm a_2 (X_o + \Delta X)^2 \pm - - - = b\sigma.$$

Thus,

$$A \frac{\partial^2(\Delta X)}{\partial t^2} + B \frac{\partial(\Delta X)}{\partial t} + C \frac{\pi^2}{l_o^2} (\Delta X) \pm 2a_2 X_o (\Delta X) = b\sigma. \quad (8)$$

In Eq. (8) higher order terms than $(\Delta X)^2$ are neglected. If we solve Eq. (8) (see Appendix II), we obtain

$$\Delta X = \frac{4b\sigma}{A\pi} \cdot \sin\left(\frac{\pi Y}{l_o}\right) \cdot \frac{e^{-\delta n}}{[(\omega_o^2 - \omega^2)^2 + (d\omega)^2]^{\frac{1}{2}}}, \quad (9)$$

where $d = B/A$, and ω_o is the resonance frequency given by

$$\omega_o = \left[\frac{1}{A}\left(C \frac{\pi^2}{l_o^2} \pm 2a_2 X_o\right)\right]^{\frac{1}{2}}$$

$$= \left(\frac{1}{A}\right)^{\frac{1}{2}} \left\{C \frac{\pi^2}{l_o^2} \pm 2a_2 \left(-\frac{l_o^2}{c\pi^2}\right) \left[K(T - T_o) \pm a_2 \frac{l_o^4}{c^2\pi^2} K^2 (T - T_o)^2 \pm - - -\right]\right\}^{\frac{1}{2}} \quad (10)$$

The resonance frequency ω_o depends on the temperature and becomes zero at a temperature T_x determined by the following equations:

$$C\frac{\pi^2}{l_o^2} - \frac{2a_2 l_o^2}{c\pi^2}\left[K(T_x - T_o) + a_2\frac{l_o^4}{c^2\pi^2}K^2(T_x - T_o)^2 + - - -\right] = 0 \qquad (11)$$

for the martensitic transformation, and

$$C\frac{\pi^2}{l_o^2} + \frac{2a_2 l_o^2}{c\pi^2}\left[K(T_x - T_o) - a_2\frac{l_o^4}{c^2\pi^2}K^2(T_x - T_o)^2 - - - -\right] = 0 \qquad (12)$$

for the reverse transformation.

Neglecting higher order terms and solving these equations, we obtain

$$T_x = T_o \pm (\sqrt{3} - 1)\frac{c^2\pi^2}{a_2 l_o^4 K}, \qquad (13)$$

where the positive sign applies to the martensitic transformation and the negative sign to the reverse transformation.

It is proposed here that the temperature T_x at which ω_o becomes zero is the M_s and A_s temperatures at which the martensitic and the reverse transformation start.

C. OBSERVATION OF THE VELOCITY CHANGE OF THE ULTRASONIC WAVE

The relative change of the velocity of the ultrasonic wave, $(\Delta V/V)$, due to the motion of half dislocation is given by

$$\frac{V_T - V}{V} = \left(\frac{\Delta V}{V}\right)_{dis} = -\frac{4NGb^2}{A\pi^2}\cdot\frac{\omega_o^2 - \omega^2}{(\omega_o^2 - \omega^2)^2 + (d\omega)^2} \qquad (14)$$

(see Eq. (AII-18) in Appendix II), where ω_o is given by Eq. (10), ω is the angular frequency of the ultrasonic wave, and N is the dislocation density.

It can be seen from Eq. (14) that the relative velocity change $(\Delta V/V)_{dis}$ will decrease as ω_o approaches ω if $\omega<\omega_o$. The frequency of the ultrasonic wave used in this experiment is of the order of kilocycles while ω_o is of the order of megacycles at the temperatures far from the transition temperature. Hence, ω_o approaches ω with $\omega<\omega_o$. Since Eq. (10) predicts that ω_o decreases as the temperature approaches A_s and M_s, it is expected from the model presented in the previous section that $(\Delta V/V)_{dis}$ will decrease (magnitude of $(\Delta V/V)_{dis}$ will increase) as the temperature approaches M_s or A_s, as shown in Figure 1. Such a decrease of the ultrasonic wave velocity was reported by Fisher and Dever[30] near the transition temperature in pure cobalt, and the same observation was made by Duggin and Rachinger[31] in $AuCuZn_2$. However, the model proposed here is valid only for the temperatures above M_s and below A_s, because the total lattice deformation accompanying the martensitic transformation cannot be described by a simple shear caused by the sweeping of a stacking fault, after the actual transformation starts.

The relative velocity change of the ultrasonic wave is related to the relative change of PRF through

$$\frac{f_T - f}{f} = \frac{\Delta f}{f} = \frac{V_T}{\ell_T} \cdot \frac{\ell}{V} - 1$$

$$= \frac{(V + \Delta V)\ell - (\ell + \Delta\ell)V}{(\ell + \Delta\ell)V}$$

$$= \frac{\Delta V}{V} - \frac{\Delta\ell}{\ell} \quad (\because \Delta\ell << \ell) \tag{15}$$

Since ΔV is consisting of ΔV due to the change of elastic constant and ΔV due to the dislocation motion, we have

$$\frac{\Delta f}{f} = \left(\frac{\Delta V}{V}\right)_{el} + \left(\frac{\Delta V}{V}\right)_{dis} - \left(\frac{\Delta\ell}{\ell}\right) , \tag{16}$$

where $(\Delta\ell/\ell)$ is the relative length change of the specimen.

As $(\Delta V/V)_{el}$ and $(\Delta\ell/\ell)$ are linearly dependent on the temperature,[38,39,42] $(\Delta V/V)_{dis}$ will be easily identified as shown in Figure 2.

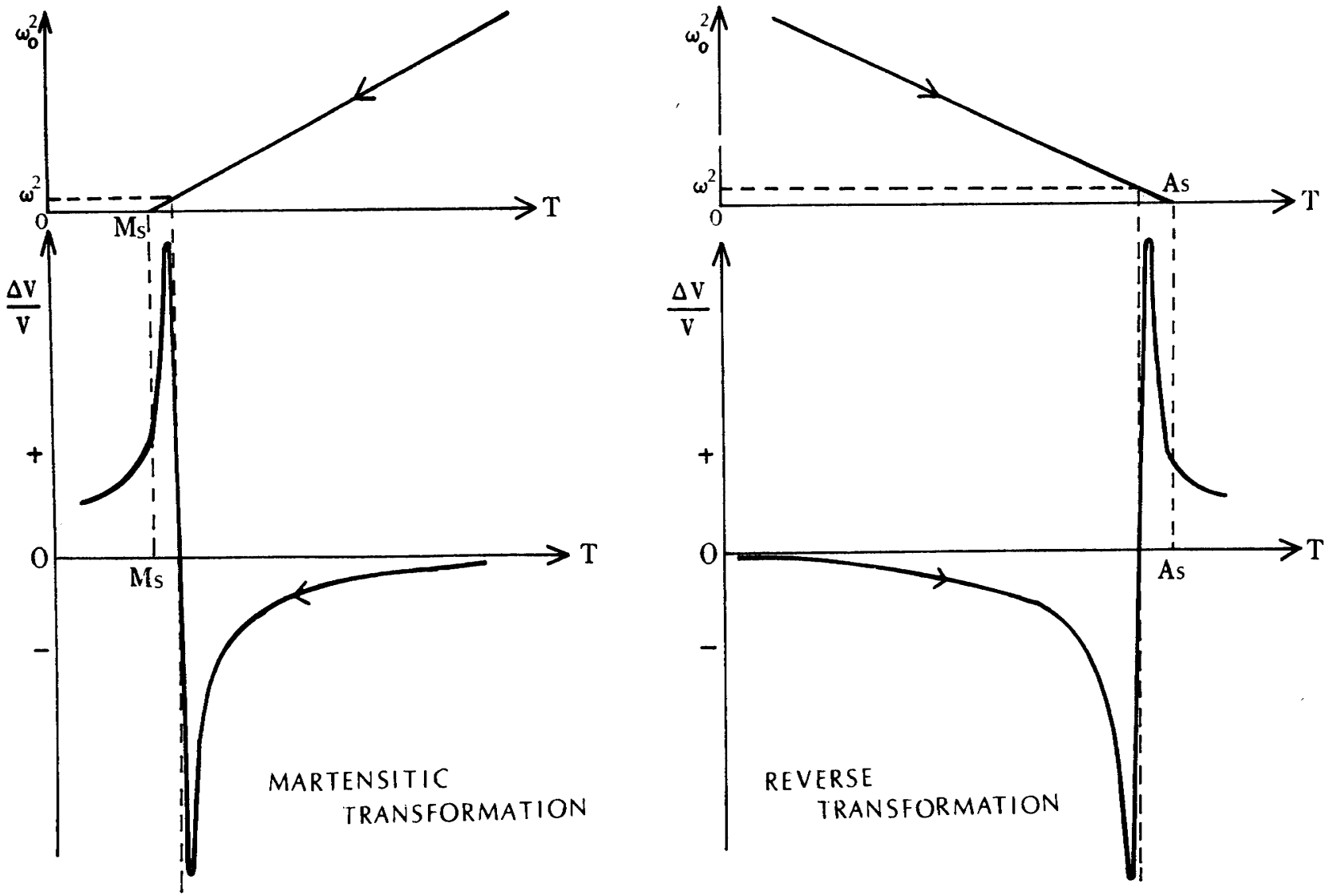

Figure 1. Temperature Dependence of ω_o^2 and $(\Delta V/V)_{dis}$ (schematic)

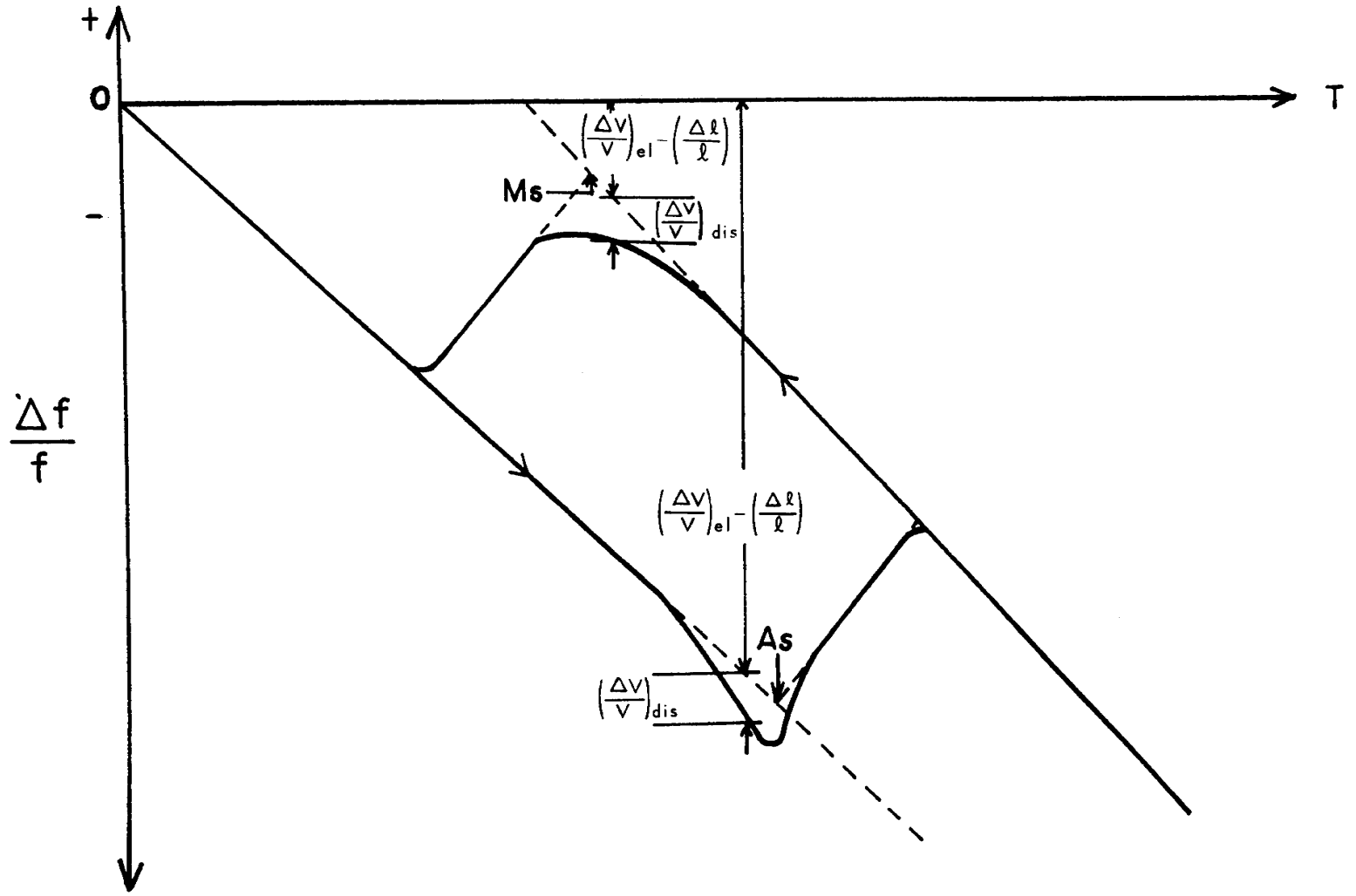

Figure 2. Prediction of Δf/f vs. Temperature (schematic)

III. EXPERIMENTAL PROCEDURE

A. ULTRASONIC MEASUREMENT

An ultrasonic pulse superposition method[32,33] was used for the velocity measurements in the wire-like specimens.[34] Figure 3 shows a schematic diagram of the apparatus for the method employed. In this arrangement, a specimen joined to the magnetostrictive drive wire by careful brazing was inserted into a quartz tube and placed in a furnace to measure the sound velocity as a function of temperature.

A typical and simple pulse echo pattern for an arbitrary input pulse repetition time (PRT) is shown in Figure 4, where the specimen is not joined to the drive wire. The 1st, 2nd, 3rd - - - round-trips of the ultrasonic pulse wave through the drive wire produce 1st, 2nd, 3rd, - - - echos respectively.

Consider now the case where the PRT of the oscillator is adjusted so that 2nd input pulse will be superimposed on the Nth echo of the 1st input pulse, as shown in Figure 5. In this case the 2nd input pulse is produced at the same time when the 1st input pulse makes N round-trips through the drive wire, and a maximum echo amplitude is observed. Consequently, the velocity of the ultrasonic wave in the drive wire can be determined from the adjusted PRT by the relationship:

$$\text{Velocity} = \frac{2 \times (\text{length of drive wire}) \times N}{(\text{PRT})}$$

or

Velocity = 2N x (length of drive wire) x (PRF),

where PRF is the pulse repetition frequency, the reciprocal of the PRT.

Figure 6 shows a more complicated pulse echo pattern pertaining to the situation where the specimen is joined to the drive wire. In this figure a large number of new echos, which are absent in Figures 4 and 5, appear. They are the result of multiple reflections at the end of specimen and at the joint of the drive wire and the specimen. The time interval Δt in Figure 6 is therefore characteristic of the specimen and corresponds to the time required for a round-trip through the specimen only. A simple way of obtaining the ultrasonic wave velocity in the specimen from the Figure 6 is to read two PRF's at which the 2nd input pulse is superimposed on T_1 and $(T_1 + \Delta t)$, or $(T_1 + \Delta t)$ and $(T_1 + 2\Delta t)$, etc., and calculate the velocity of the ultrasonic wave in the specimen with the length ℓ from the equation:

$$V = \frac{2\ell}{\Delta t} = \frac{2\ell}{(PRT)_{T_1 + \Delta t} - (PRT)_{T_1}}$$

or

$$V = \frac{2\ell \times (PRF)_{T_1} \times (PRF)_{T_1 + \Delta t}}{(PRF)_{T_1} - (PRF)_{T_1 + \Delta t}}$$

This way of obtaining the velocity can be applied only when the temperature of the specimen does not change or

changes slowly enough to allow adjustment of the PRT to be made twice. Since such a slow temperature change cannot be expected for most measurements, a somewhat more complicated but more accurate technique requiring only one adjustment of the PRT was employed in this experiment.

As the PRT is adjusted to a relatively short time, new pulse echos begin to appear in the region between the 1st input pulse and the echo position T_1, due to the overlapping of the successive pulse echo patterns. Figure 7 shows how the resulting pulse echo pattern develops when the PRT is adjusted to be equal to $2\Delta t$. The solid lines in Figure (7-b) represent the sum of the echo amplitudes shown in Figure (7-a). Since the pulse echo patterns are continued infinitely, the dotted lines in Figure (7-b) should be also observed, resulting in a maximum echo amplitude as shown in Figure (7-c).

As the temperature of the specimen changes, Δt will change accordingly due to the velocity change of the ultrasonic wave and the echo amplitude will decrease thereon. The readjustment of the PRT necessary to maximize the echo amplitude again will give the velocity change and can be easily measured even though the temperature may change rapidly.

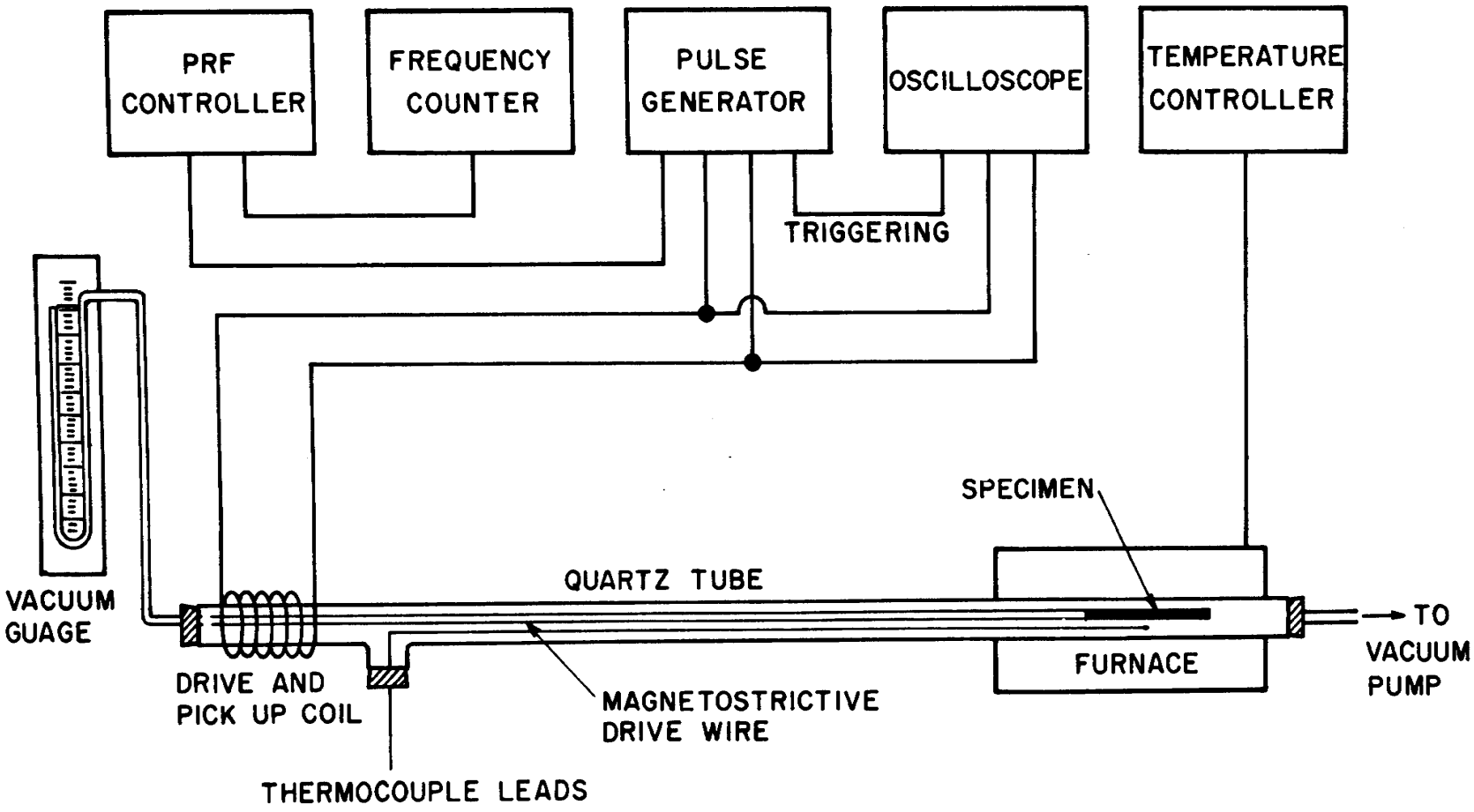

Figure 3. Schematic Diagram of the Ultrasonic Measurement

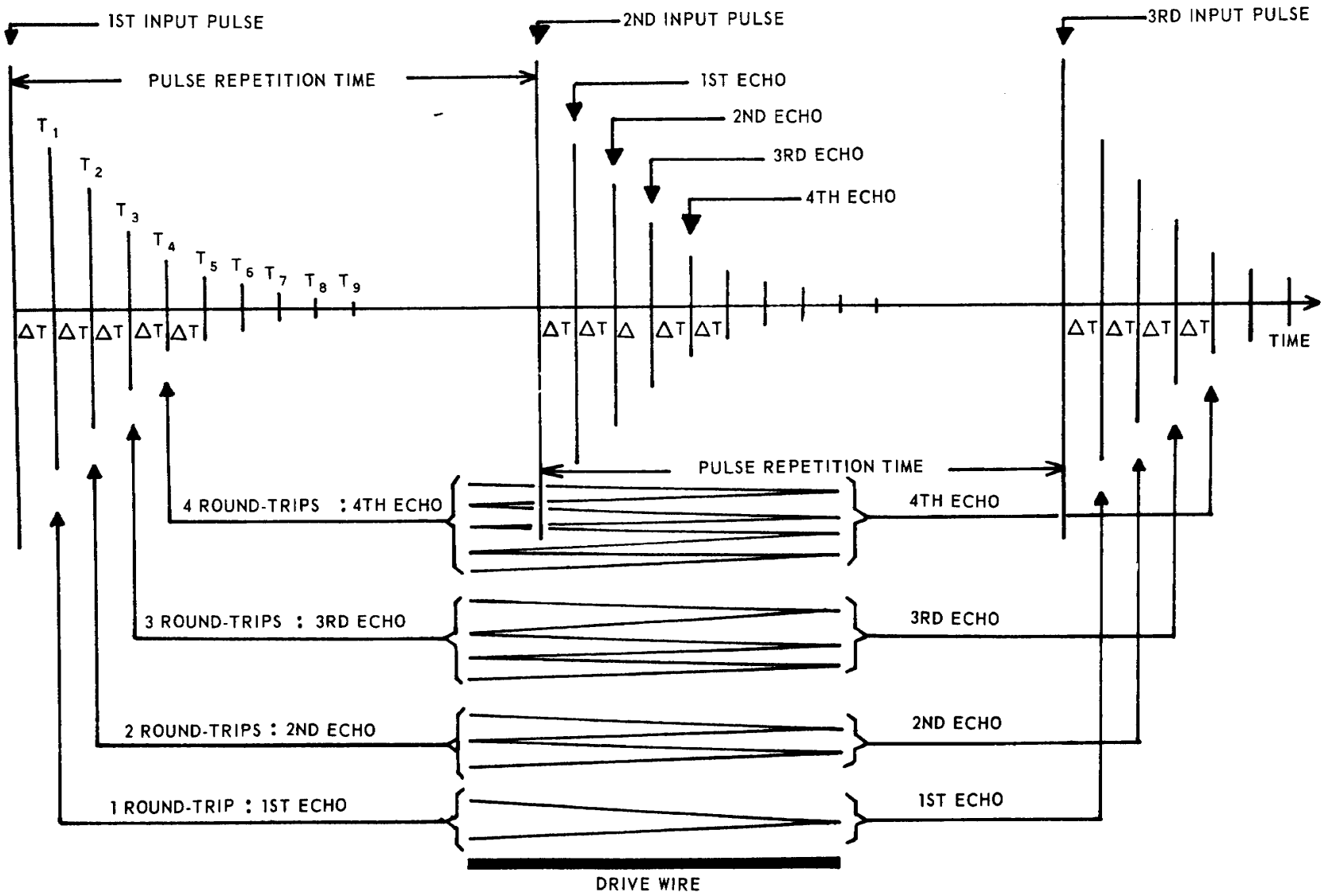

Figure 4. Typical Pulse Echo Pattern (without specimen)

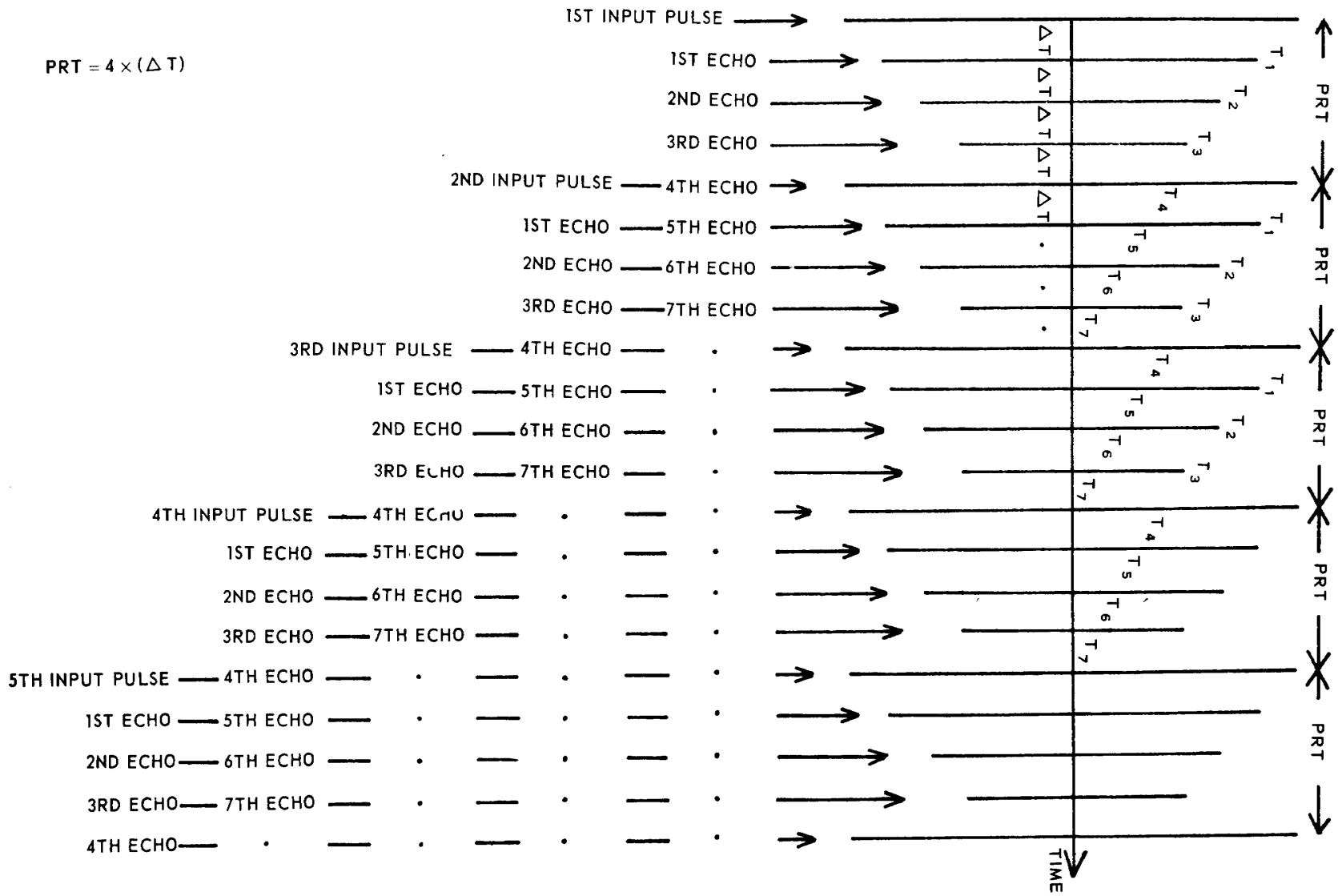

Figure 5. Pulse Echo Pattern with Adjusted PRT (without specimen)

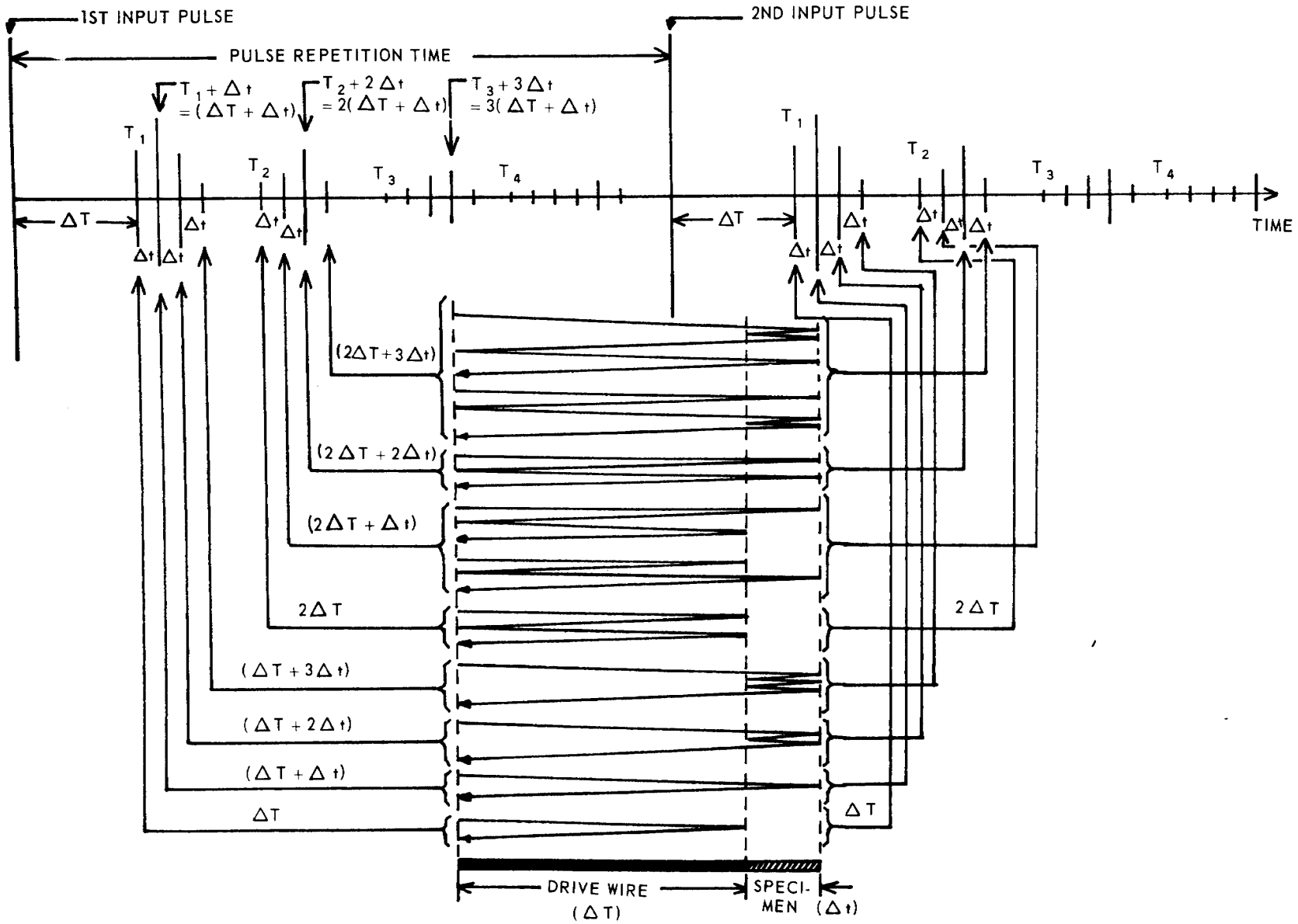

Figure 6. Typical Pulse Echo Pattern (with specimen)

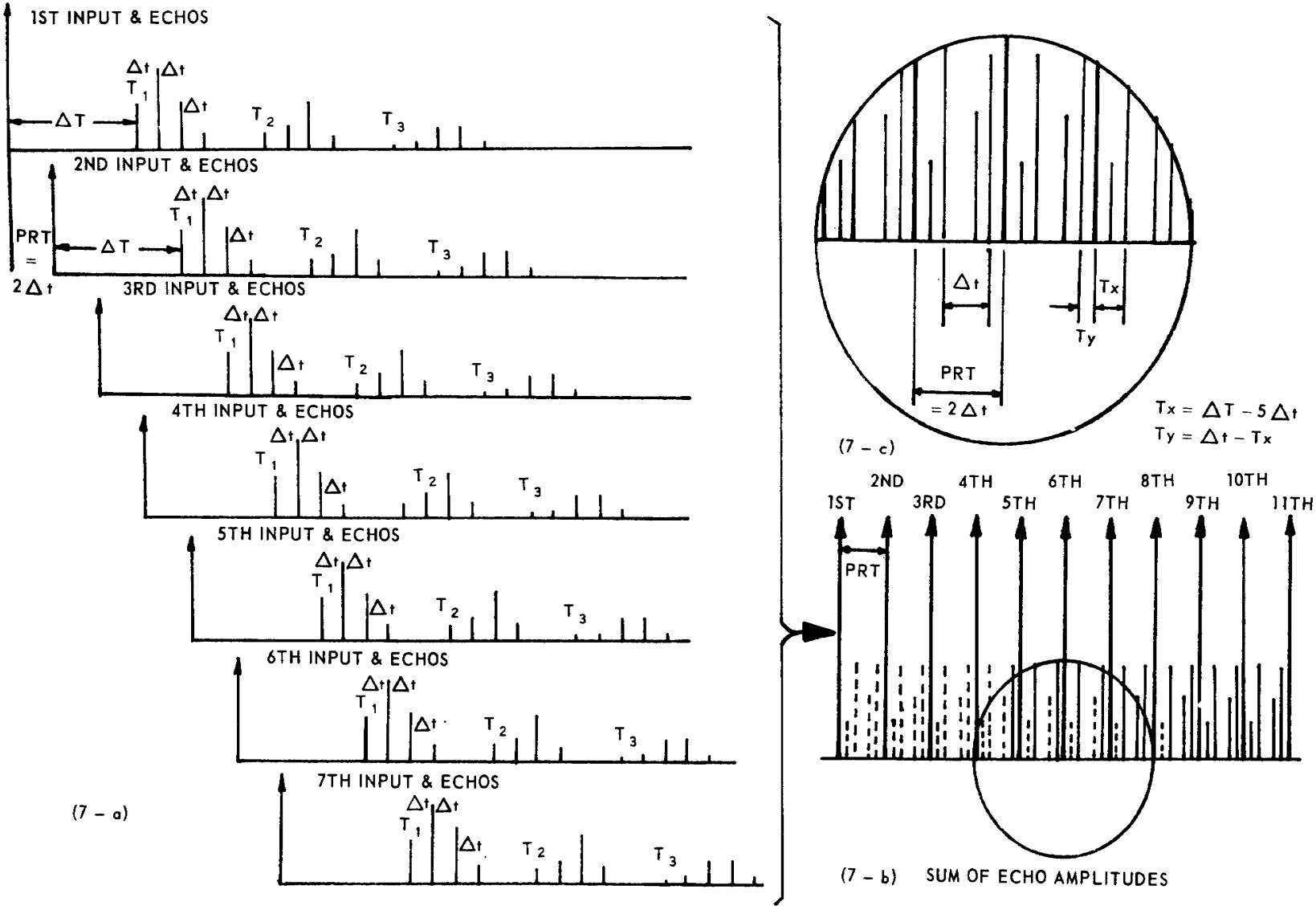

Figure 7. A Maximum Echo Amplitude when PRT=2ΔT

B. THERMAL DILATATION MEASUREMENT

Since the ultrasonic measurement ($\Delta f/f$) contains the thermal dilatation ($\Delta \ell/\ell$) of the specimen, it is necessary to measure the thermal dilatation ($\Delta \ell/\ell$) of the specimen in order to separate out the relative velocity change ($\Delta V/V$) from the relative change of PRF ($\Delta f/f$).

A Leitz dilatometer model HTV was used to measure thermal expansion of the specimens. The small dilatometric change of the specimen was transmitted by way of a quartz bar to a photographical recording system. The deviation of the dilatometric curve from the same curve of a standard body of known expansion, chronin, yields the thermal expansion of the specimen.

C. SAMPLE PREPARATION

The alloys (Fe-28.09 at.%Ni, Fe-28.34 at.%Ni, Fe-31.09 at.%Ni, Fe-31.95 at.%Ni, and Fe-33.62 at.%Ni) were prepared by melting electrolytic Fe(99.91%) and Ni(Inco 270:99.98%) in a resistance furnace in a 6" Hg helium-atmosphere. The ingots were swaged to 0.125" dia. A portion of each swaged alloy with 0.125" dia. was finished to be 50mm long for the dilatometric measurements. The remaining parts were swaged again to 0.05" dia. with repeated intermediate vacuum-anneals for the ultrasonic measurements. Prior to both measurements the specimens were vacuum-annealed at 1200°C for 24 hours and subsequently held in liquid N_2 for 10

minutes. Carbon content in the specimens was analysed to be below 0.01%.

IV. RESULTS AND DISCUSSIONS

In order to examine the prediction that $(\Delta V/V)_{dis}$ will become appreciable as the temperature approaches A_s, five Fe-Ni specimens with different compositions were run in this experiment. Figures 8 to 12 show the observed relative change of PRF of the ultrasonic wave as a function of temperature. In these figures (except Figure 12) an agreement with the prediction given by Figure 2 is observed. However, to clarify the effect due to the dislocation motion it is necessary to know $(\Delta V/V)$ where $(\Delta \ell/\ell)$ is eliminated.

The relative length changes of five Fe-Ni alloys obtained by dilatation measurement are shown in Figures 13 to 17. The Fe-28.09%Ni, Fe-28.34%Ni, and Fe-31.09%Ni specimens show thermal expansion curves displaying the reverse (martensitic) transformation. On the other hand, thermal expansion curves for Fe-31.95%Ni and Fe-33.62%Ni specimens show no indication of the phase transformation, due to the fact that M_s temperature for Fe-31.95%Ni is near -120°C and no martensitic phase for Fe-33.62%Ni can be obtained by quenching.[35] It is believed that the martensitic transformation of Fe-31.95%Ni specimen was incomplete.

Figures 18 to 20 show the velocity change of the ultrasonic wave for Fe-28.09%Ni, Fe-28.34%Ni, and Fe-31.09% Ni specimens obtained from the frequency change and the length change by means of the relation given by Eq. (15), where usually ΔV and Δf are negative and $\Delta \ell$ is positive. Since $(\Delta V/V)$ consists of $(\Delta V/V)_{el}$ and $(\Delta V/V)_{dis}$, the

deviation from the straight line in Figures 18 to 20 is identified as $(\Delta V/V)_{dis}$.

The data for Fe-31.95%Ni cannot be explained in this fashion because the ratio of the transformed martensite phase and the untransformed austenite phase could not be determined. Data for Fe-33.62%Ni show that $(\Delta V/V)$ increases up to 250°C and begins to decrease above 250°C. The temperature where $(\Delta V/V)$ has a maximum value is identified as the Curie temperature T_c for Fe-33.62%Ni (austenite phase).[36]

Turning back to the results obtained from Fe-28.09%Ni, Fe-28.34%Ni, and Fe-31.09%Ni which are the only useful ones for the presented model on the reverse transformation, it is observed that $(\Delta V/V)_{dis}$ becomes more and more appreciable as the temperature increases to A_s, as predicted. This decrease of the ultrasonic velocity indicates that there is an anomalous decrease of elastic constant beyond the usual linear relationship between the elastic constant and the temperature:

$$\left(\frac{\Delta V}{V}\right)_{el} = \frac{\sqrt{(G + \Delta G)(\upsilon + \Delta\upsilon)} - \sqrt{G\upsilon}}{\sqrt{G\upsilon}}$$

$$= (1 + \frac{\Delta G}{G})^{\frac{1}{2}} (1 + \frac{\Delta\upsilon}{\upsilon})^{\frac{1}{2}} - 1$$

$$\simeq \frac{1}{2}\frac{\Delta G}{G} + \frac{1}{2}\frac{\Delta\upsilon}{\upsilon}$$

or

$$\frac{\Delta G}{G} = 2\left(\frac{\Delta V}{V}\right)_{el} - 3\left(\frac{\Delta \ell}{\ell}\right)$$

where $V = (G/\rho)^{\frac{1}{2}} = (G\upsilon)^{\frac{1}{2}}$, G is the elastic constant, and $\upsilon = 1/\rho$ is the specific volume of the specimen.

This anomalous decrease of the ultrasonic velocity near the A_s temperature can be interpreted in the following way.

1) The velocity change due to the dislocation motion is a function of ω_o (see Eq. (14)). At temperatures sufficiently low from A_s, $(\Delta V/V)_{dis}$ is expected to change slowly, while near the A_s temperature $(\Delta V/V)_{dis}$ decreases appreciably.
2) The appreciable decrease of $(\Delta V/V)_{dis}$ near the A_s temperature reflects the instability of dislocation and causes the anomalous decrease of the ultrasonic velocity.
3) Since ω_o is inversely proportional to the distance between the pinning points, the amount of $(\Delta V/V)_{dis}$ depends on the dislocation loop length as well as temperature.

One of the difficulties in studying the reverse transformation is that the small amount of carbon which is inevitably present in the ferric alloys aggregates during heating[40] and the tempering effect appears. Thus it might be suggested that the anomalous decrease of the ultrasonic

velocity is due to the tempering effect. However, the carbon aggregates must be expected to be barriers to the dislocation motion and thus should cause an increase of elastic constant, i.e., an increase of the ultrasonic velocity. Consequently, the observed anomalous decrease of the ultrasonic velocity cannot be due to the tempering effect, but it can be said that the effect of the dislocation motion may be reduced somewhat due to the tempering effect. Thus, reducing the carbon content and relatively fast heating are necessary to reduce the tempering effect as low as possible. In this experiment carbon content was held below 0.01% and heating rate was chosen to be 5°C per minute.

It should also be pointed out that the reverse transformation accompanies a magnetic transformation from the ferromagnetic martensite phase to the paramagnetic austenite phase,[43] as the Curie temperature of the Fe-Ni austenite phase is lower than the temperature A_f where the reverse transformation completes. This magnetic transformation, however, cannot give rise to a decrease in $(\Delta V/V)$. It rather results in a increase of $(\Delta V/V)$ if the measurements are performed in zero (the earth's) magnetic field[39] as was done in this experiment. This is reflected also by the increase of $(\Delta f/f)$ at temperatures between A_s and A_f (see Figures 8, 9, and 10).

In summary, then, the present data support the hypothesis of a dislocation instability triggering the

martensitic and the reverse martensitic transformation as do previous data on Co[30], Fe-28%Ni[41], and $AuCuZn_2$.[31]

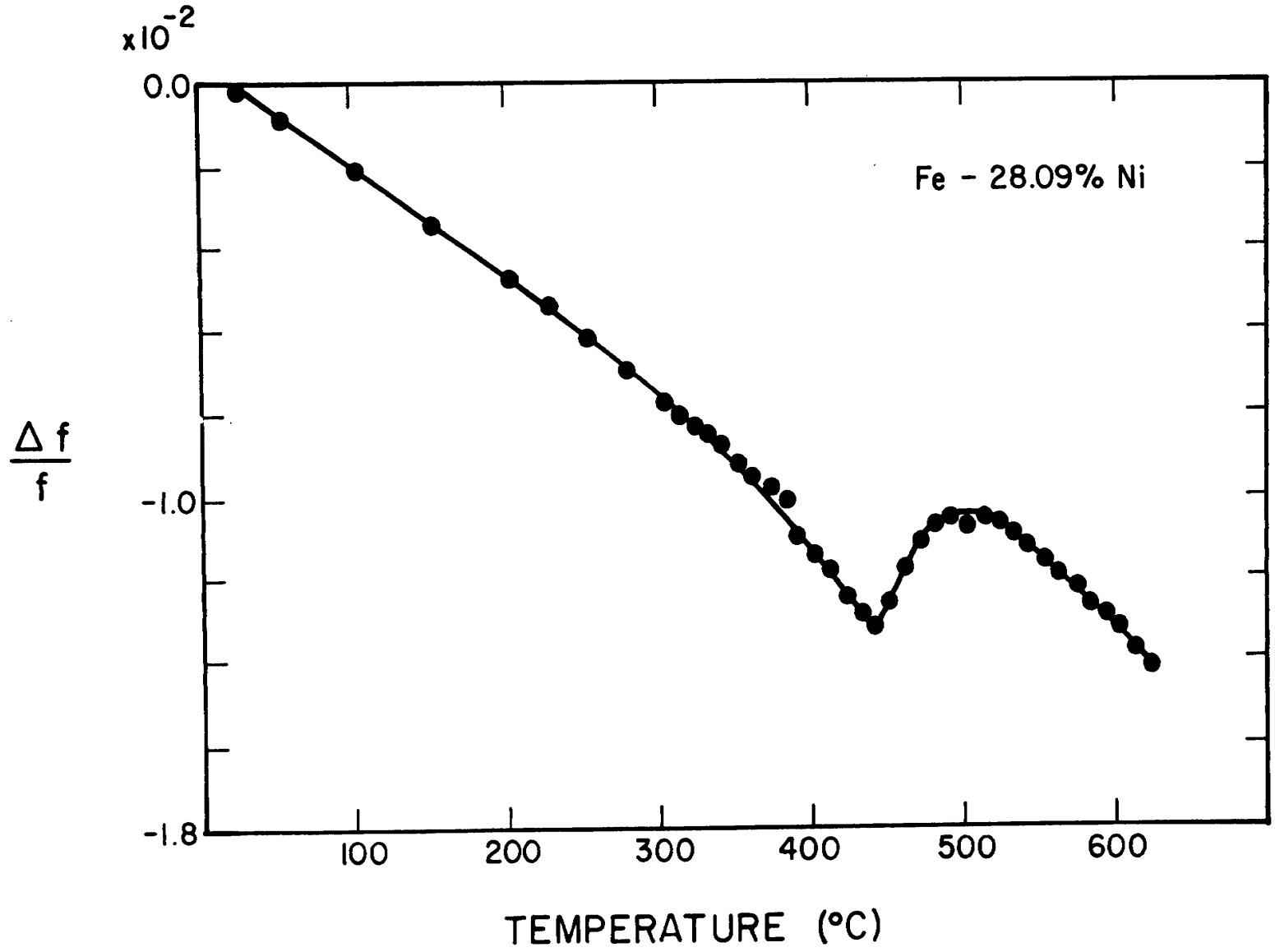

Figure 8. Relative Change of PRF for Fe-28.09%Ni Specimen

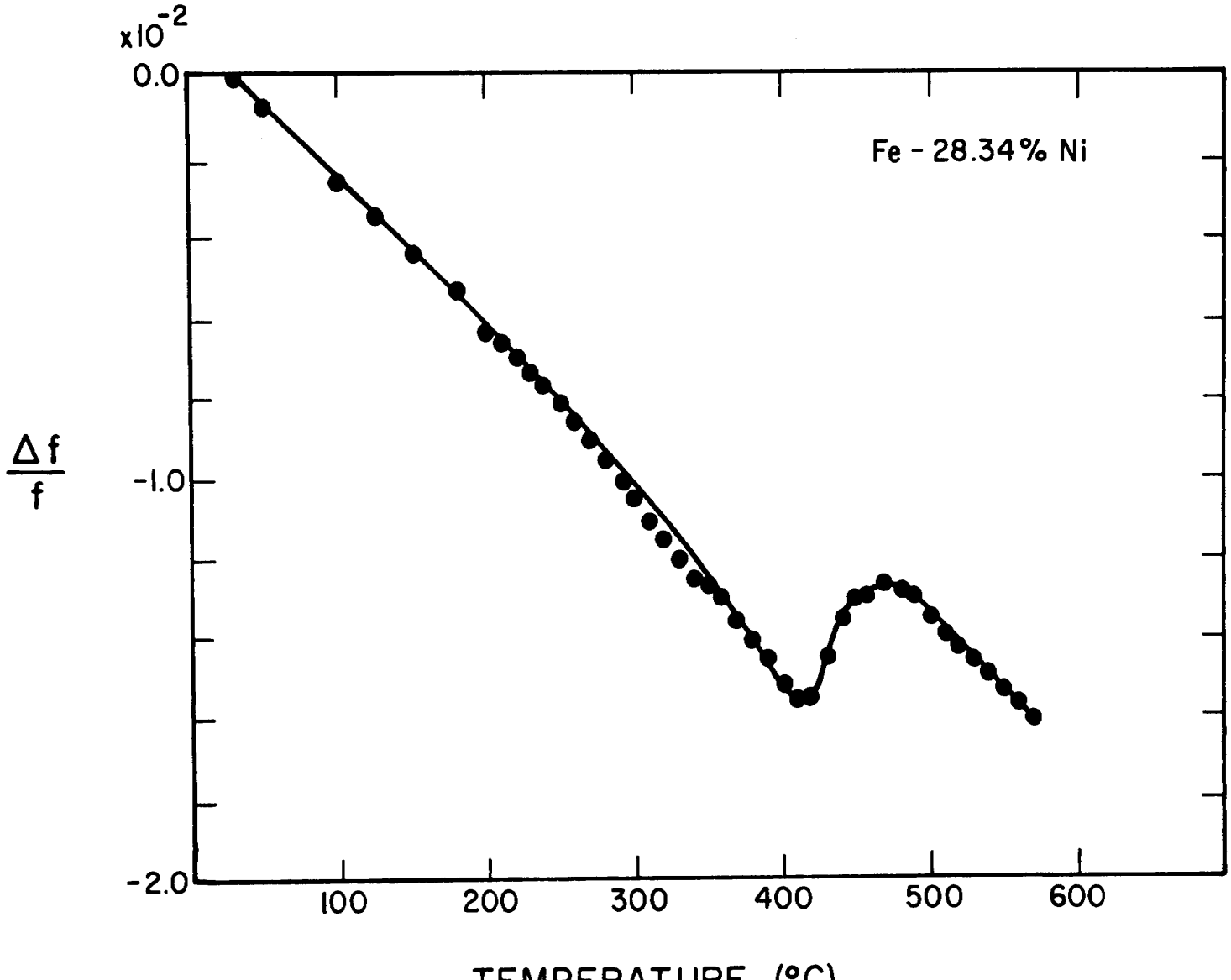

Figure 9. Relative Change of PRF for Fe-28.34%Ni Specimen

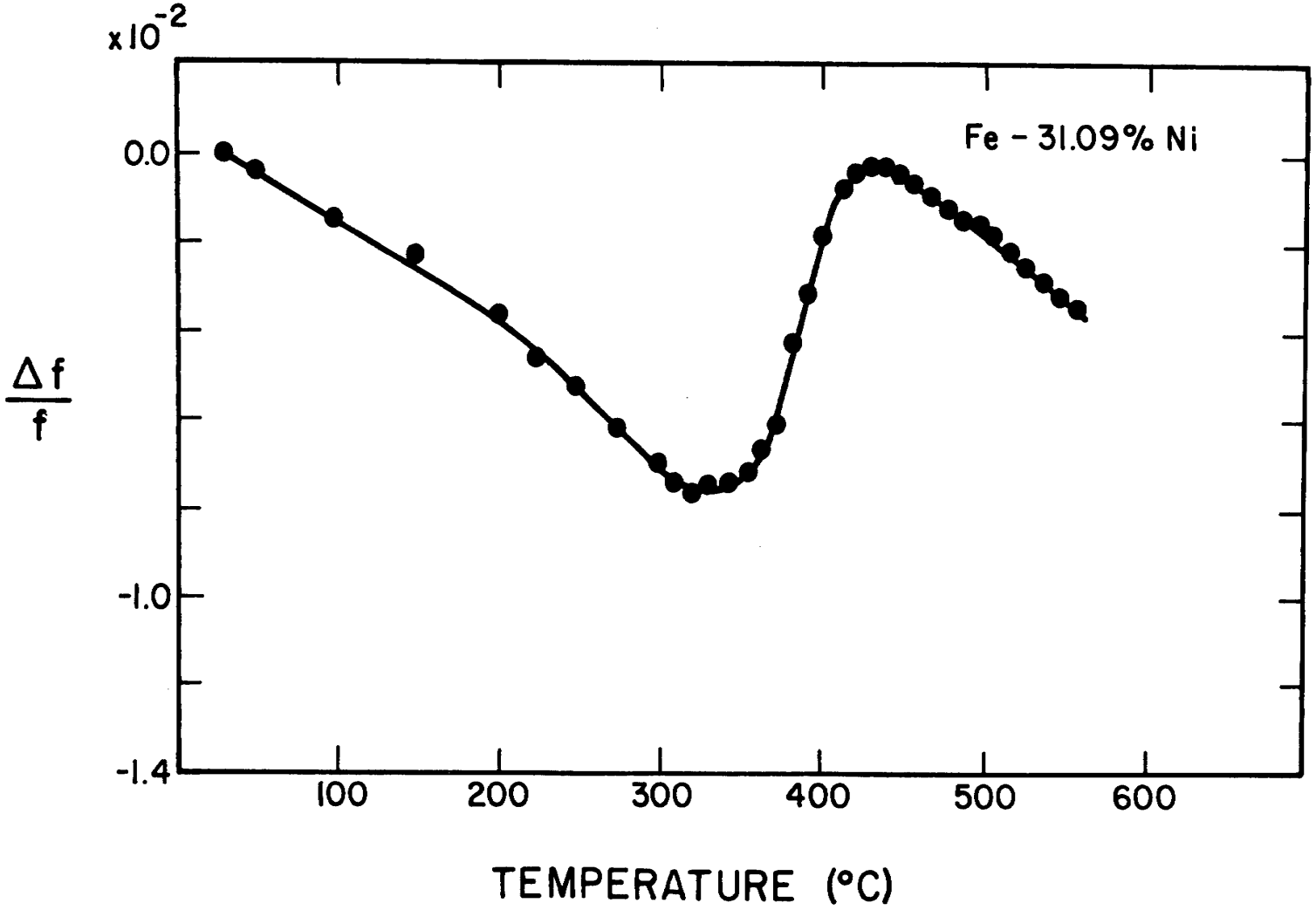

Figure 10. Relative Change of PRF for Fe-31.09%Ni Specimen

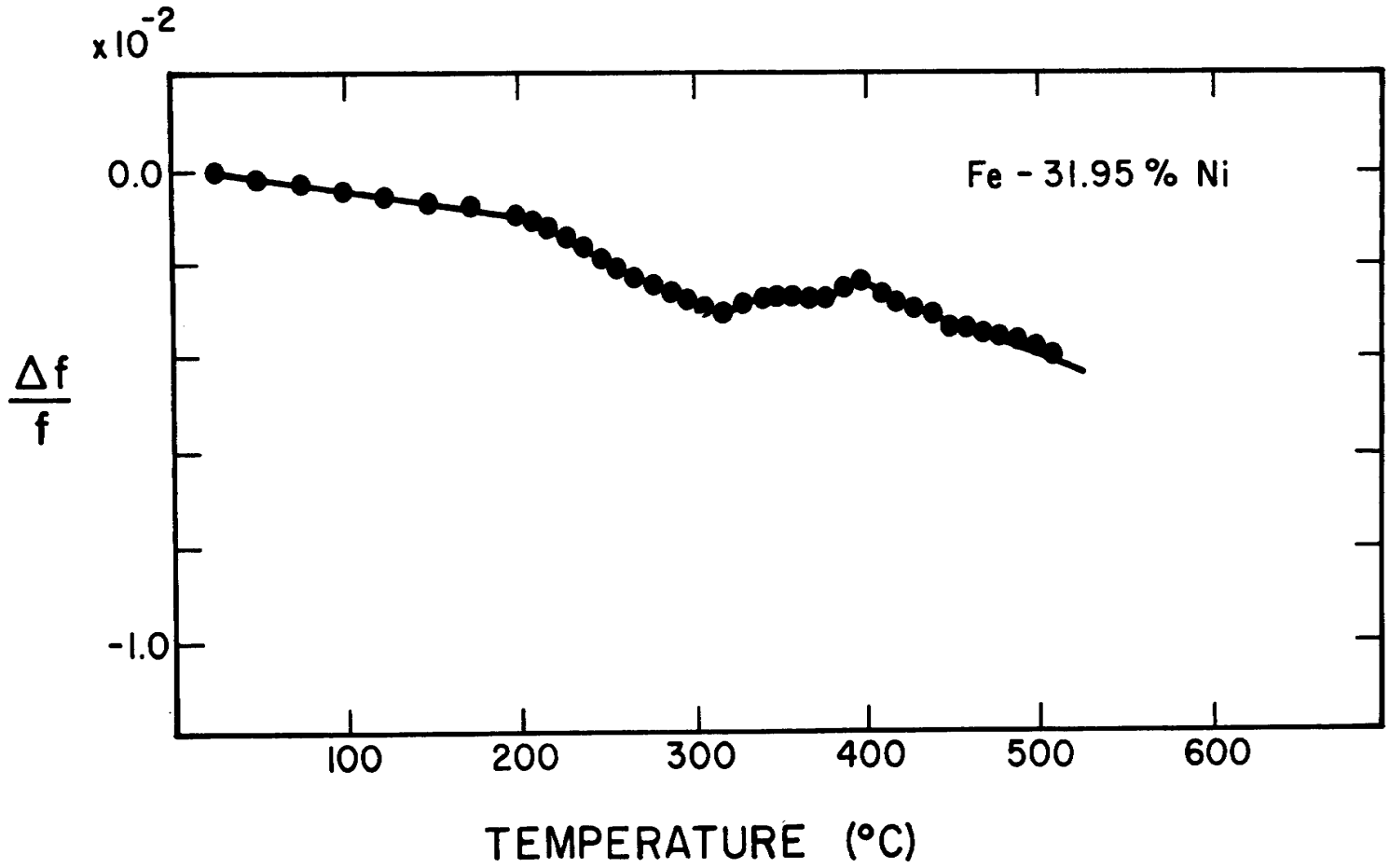

Figure 11. Relative Change of PRF for Fe-31.95%Ni Specimen

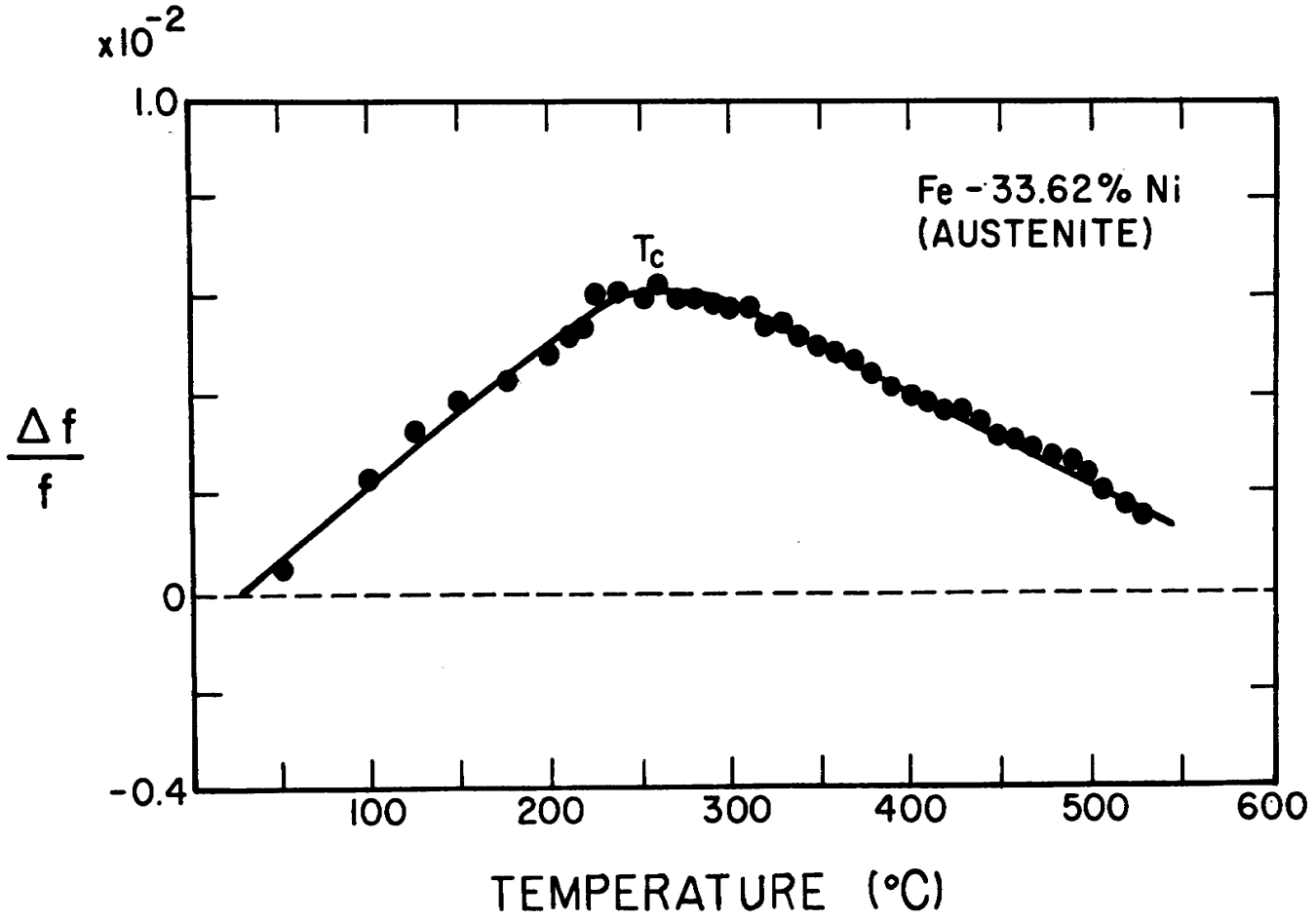

Figure 12. Relative Change of PRF for Fe-33.62%Ni Specimen

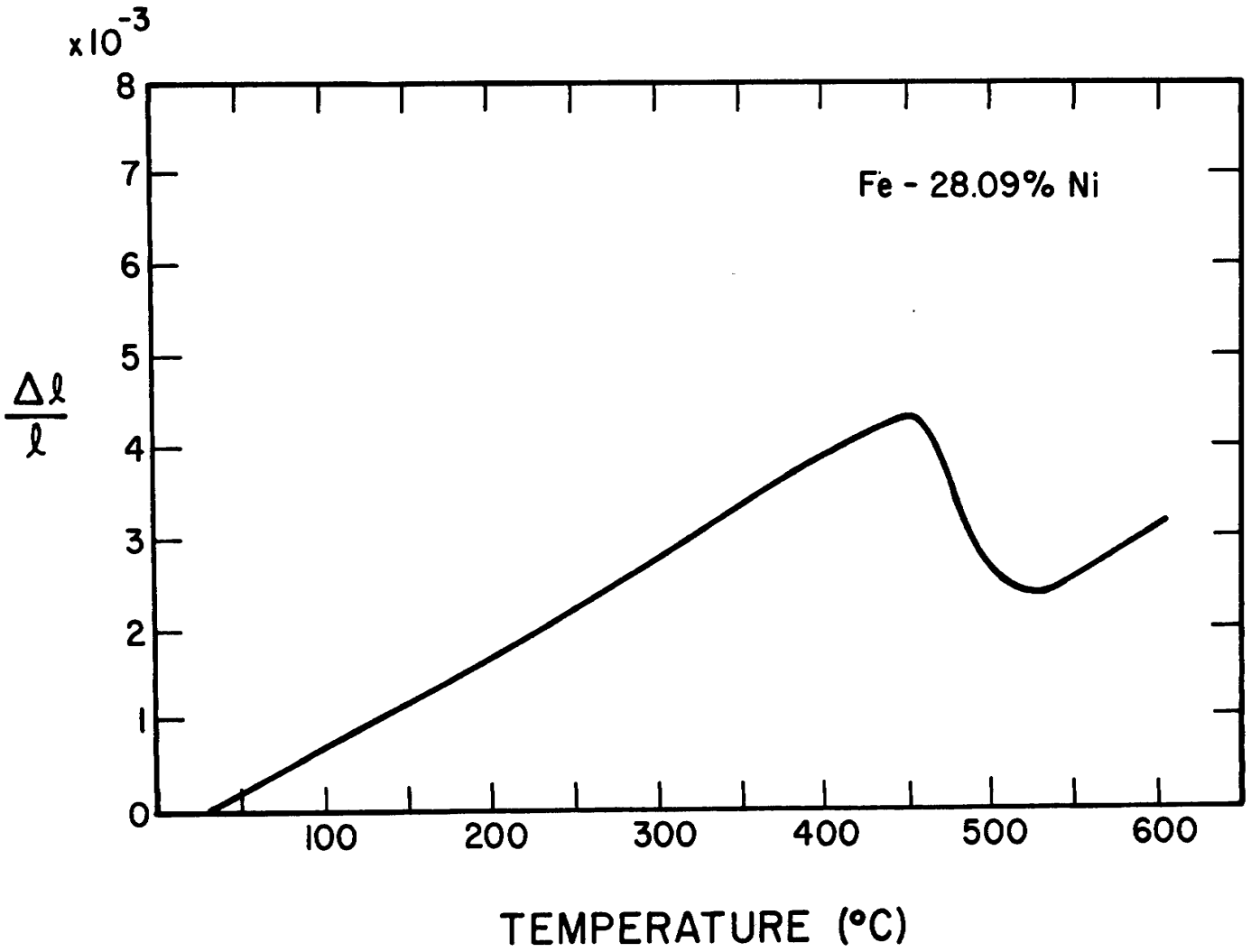

Figure 13. Relative Length Change of Fe-28.09%Ni Specimen

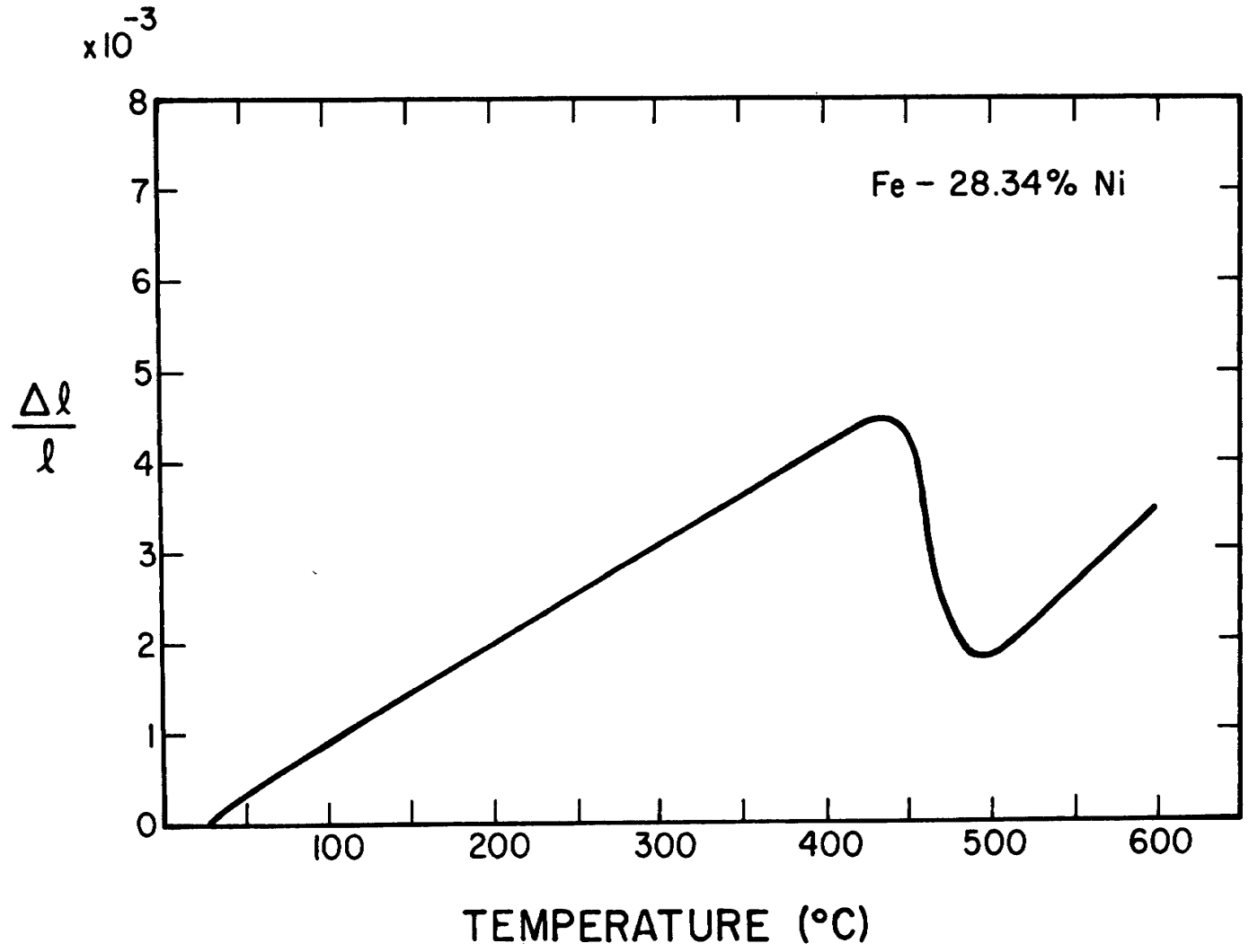

Figure 14. Relative Length Change of Fe-28.34%Ni Specimen

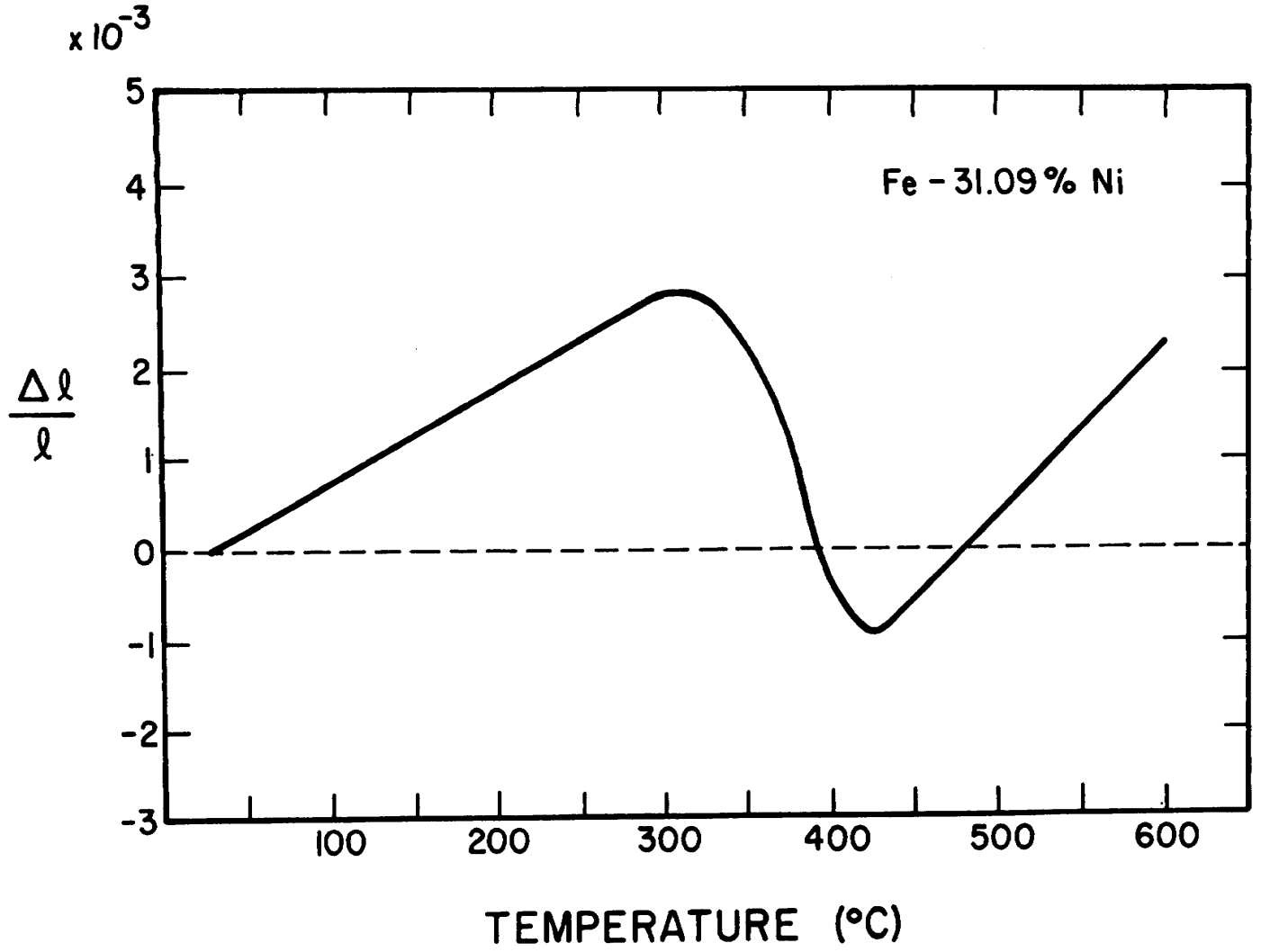

Figure 15. Relative Length Change of Fe-31.09%Ni Specimen

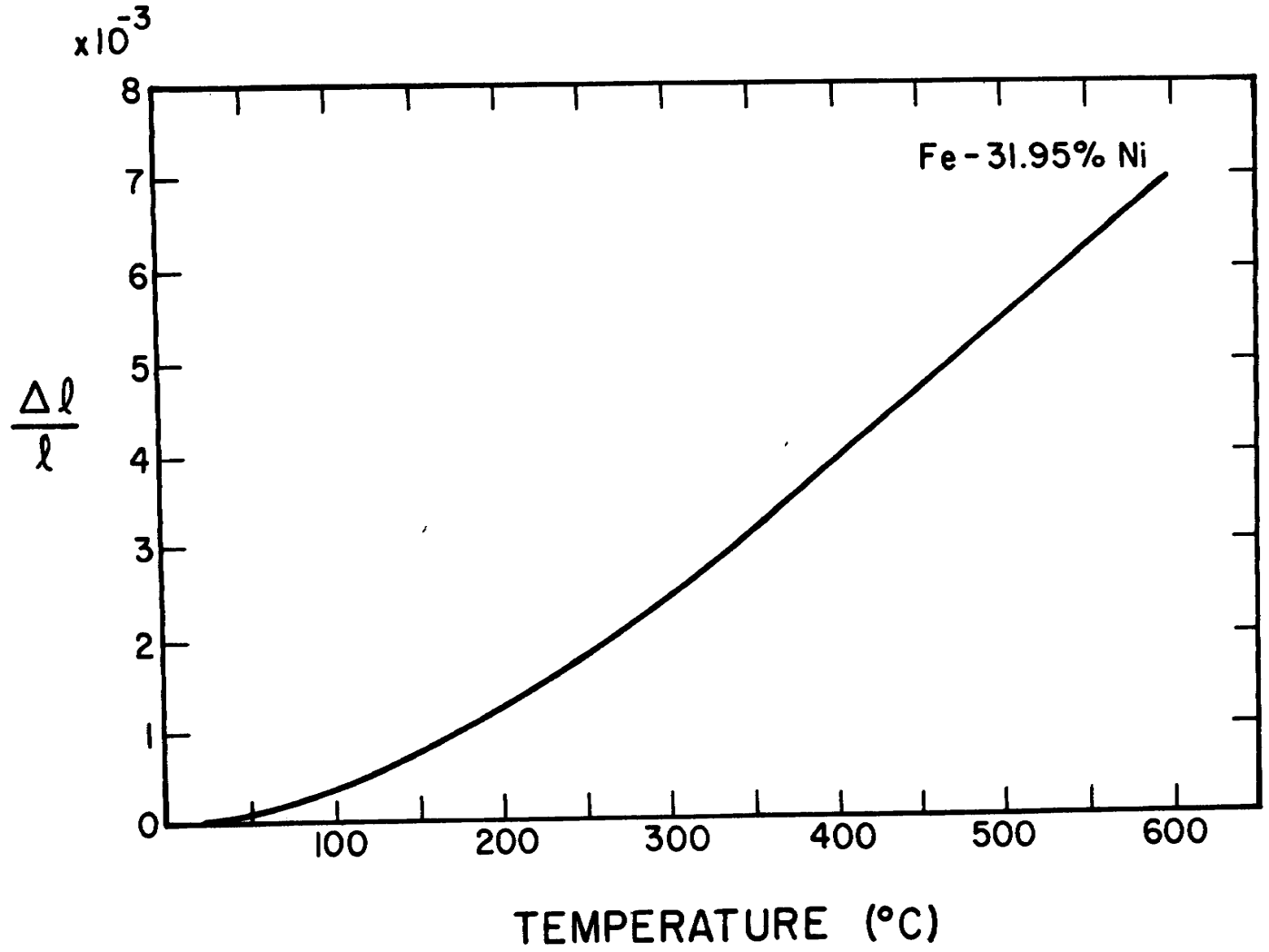

Figure 16. Relative Length Change of Fe-31.95%Ni Specimen

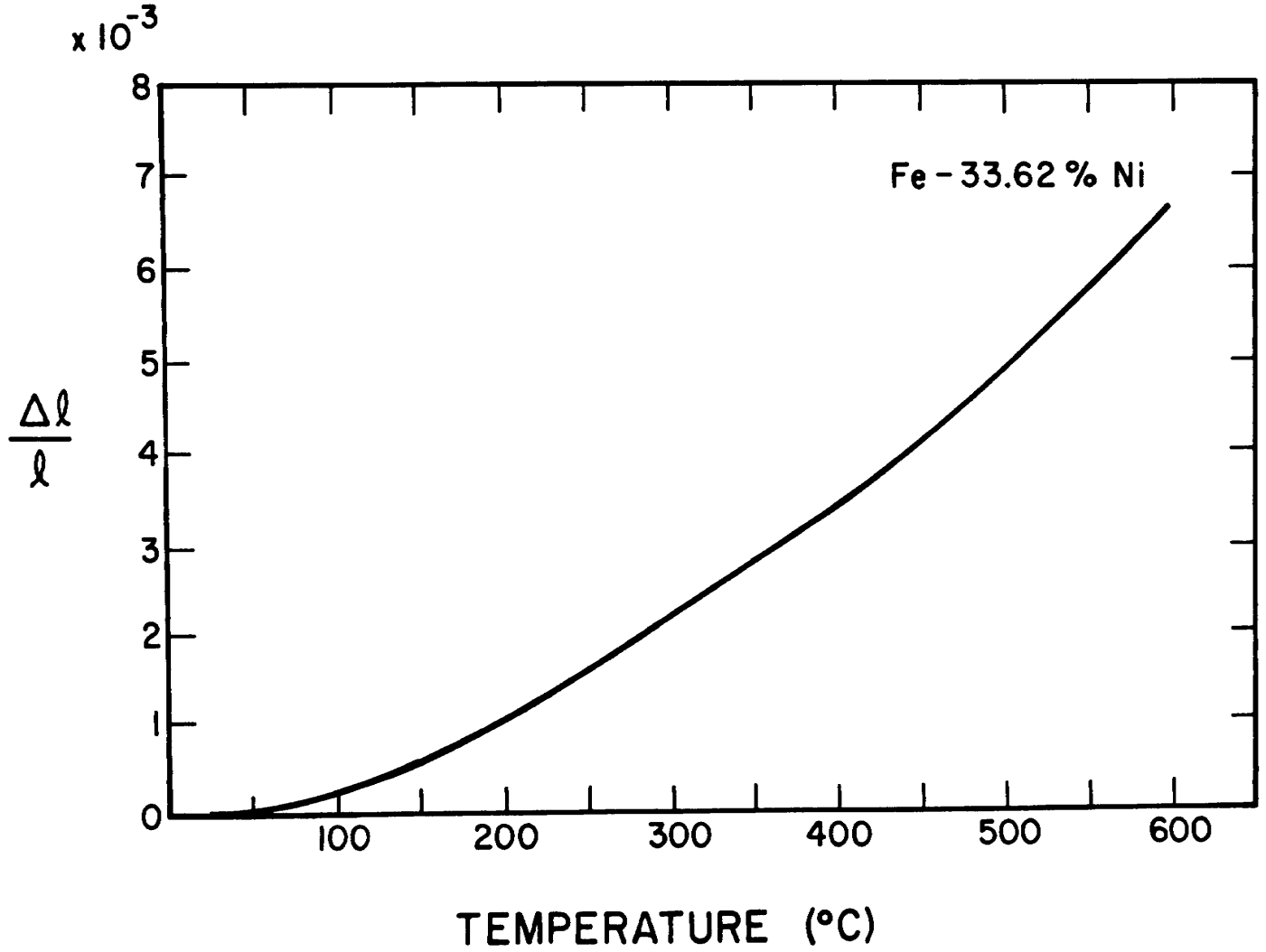

Figure 17. Relative Length Change of Fe-33.62%Ni Specimen

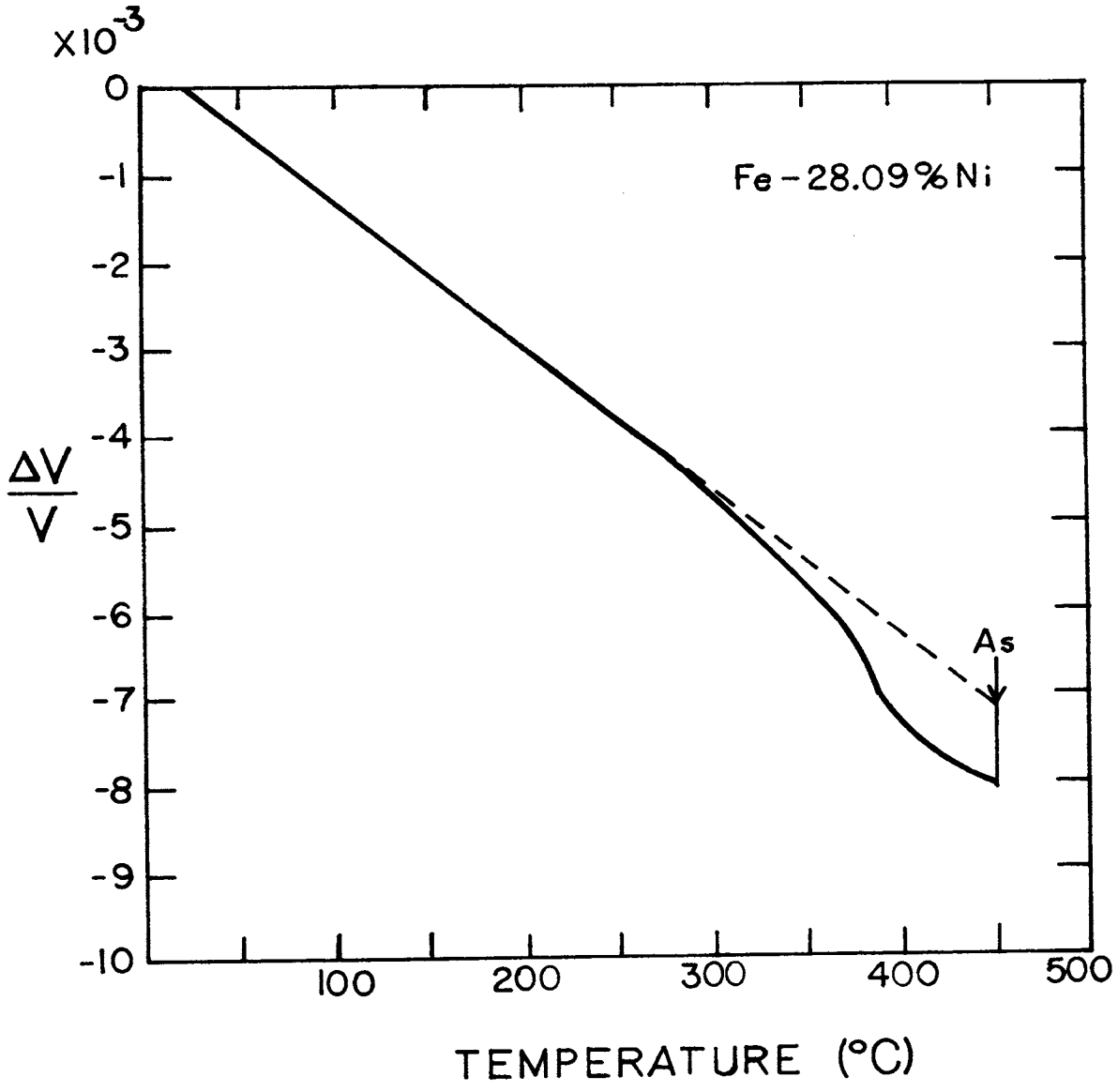

Figure 18. Relative Velocity Change of the Ultrasonic Wave for Fe-28.09%Ni Specimen

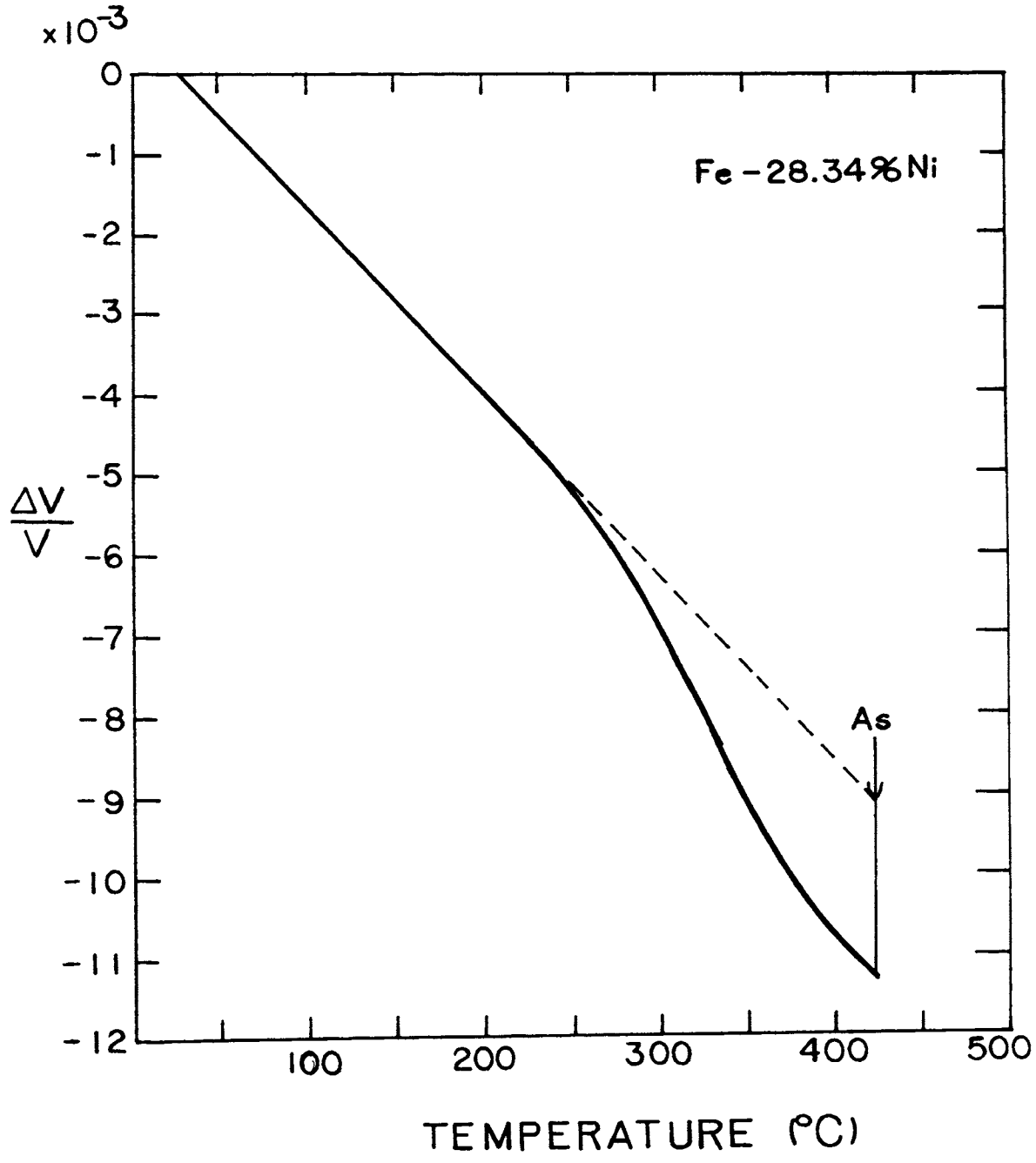

Figure 19. Relative Velocity Change of the Ultrasonic Wave for Fe-28.34%Ni Specimen

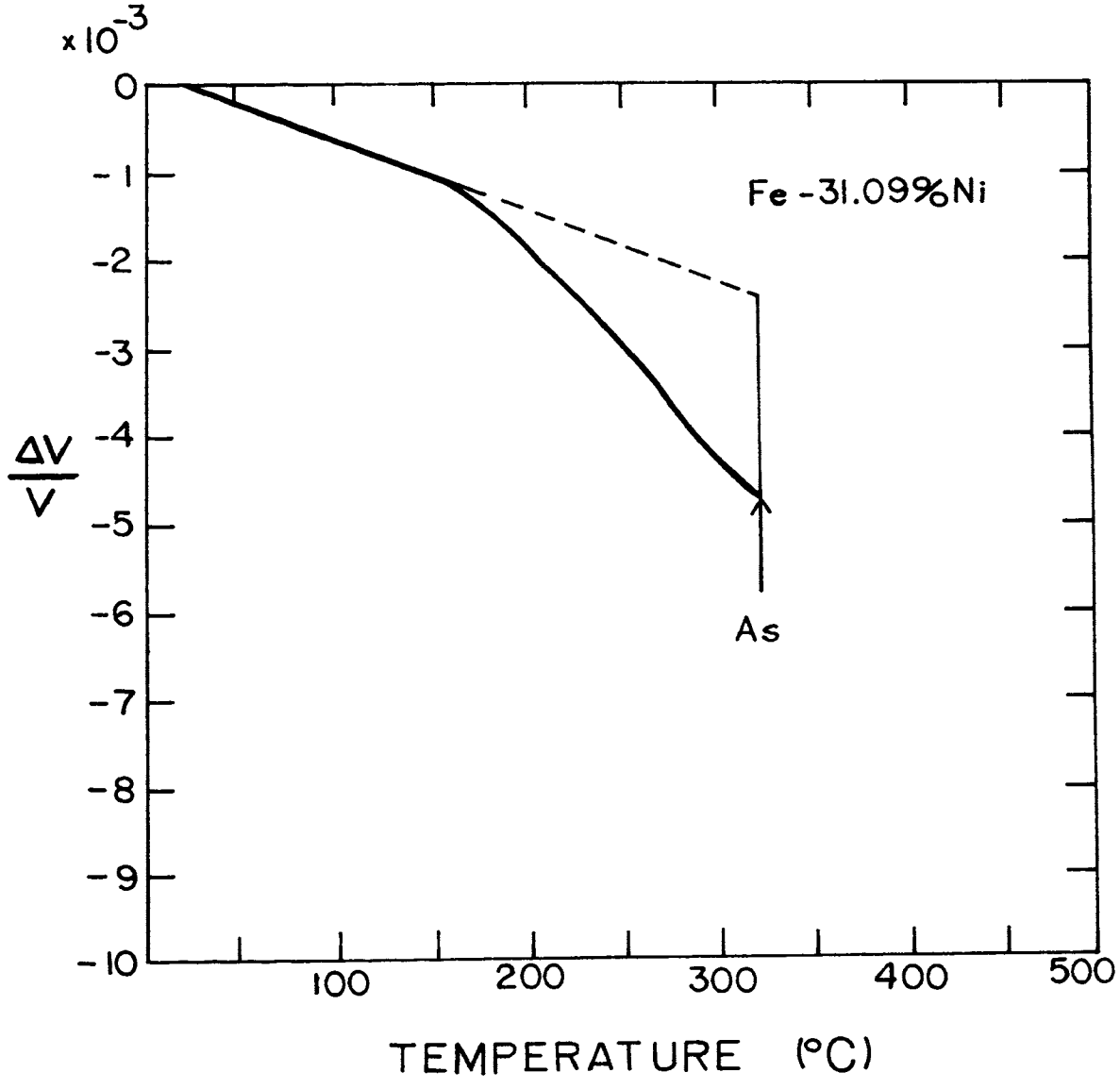

Figure 20. Relative Velocity Change of the Ultrasonic Wave for Fe-31.09%Ni Specimen

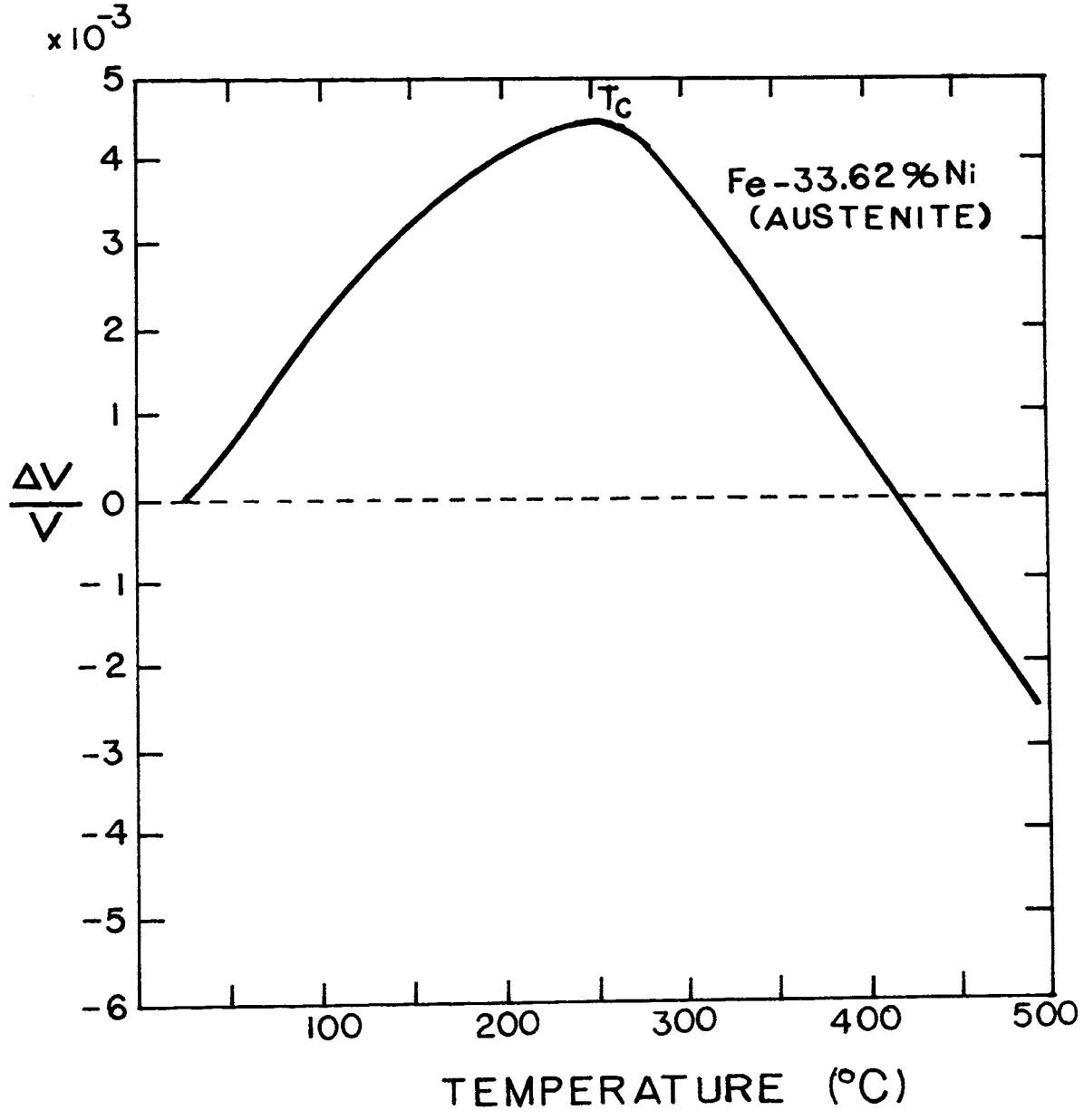

Figure 21. Relative Velocity Change of the Ultrasonic Wave for Fe-33.62%Ni Specimen

V. CONCLUSION

In this experiment an anomalous decrease of the ultrasonic sound velocity was observed in the Fe-Ni martensite phase as the temperature approaches A_s on heating.

It is concluded that the anomalous decrease of the sound velocity is due to the dislocation motion and the deviation from the linear relationship of the temperature-dependent velocity change indicates the onset of the dislocation instability.

VI. REFERENCES

1. Greninger, A. B., and Troiano, A. R., Trans. AIME, 140, 307 (1940); Ibid, 185, 590 (1949).

2. Wechsler, M. S., Liberman, D. S., and Read, T. A., Trans. AIME, 197, 1503 (1953).

3. Bowles, J. S., and Machkenzie, N. A., Acta Met., 2, 129 (1954a); Ibid, 2,224 (1954b).

4. Bowles, J. S., and Barrett, C. S., Progress in Metal Physics, vol. 3, Pergamon Press, London, 1952, p. 1.

5. Barrett, C. S., and Massalski, T. B., Structure of Metals 3rd Ed., McGraw Hill, New York, 1966, p. 517-534.

6. Kaufman, L., and Kaufman, M., Progress in Metal Physics, vol. 7, Pergamon Press, London, 1958, p. 165.

7. Christian, J. W., The Mechanism of Phase Transformations in Crystalline Solids, Inst. of Metals, London, 1969, p. 129-142.

8. Klosterman, J. A., Ibid, p. 143-151.

9. Eastering, K. E., and Swann, P. R., Ibid, p. 152-155.

10. Entwisle, A. R., and Feeney, J. A., Ibid, p. 156-161.

11. Lieberman, D. S., Ibid, p. 167-175.

12. Waymann, C. M., Introduction to the Crystallography of Martensitic Transformation, MacMillan, New York, 1964.

13. Christian, J. W., The Theory of Transformation in Metals and Alloys, Pergamon Press, London, 1965, p. 802-931.

14. Scheil, E. Z., A. Anorg. Chem., 207, 21 (1932).

15. Chang, L. C., and Read, T. A., Trans. AIME, 191, 47 (1951).

16. Zener's Interpretation was quoted by MacReynolds, A. W., J. Appl. Phys., 20, 896 (1949).

17. Christian, J. W., Proc. Roy. Soc., A206, 51 (1951).

18. Jaswon, M. A., The Mechanism of Phase Transformation in Metals, Inst. of Metals, London, 1956, p. 173.

19. Cohen, J. B., Hinton, R., Lay, K., and Sara, S., Acta Met., 10, 894 (1962).

20. Ericsson, T., Acta Met., 14, 853 (1966).

21. Read, T. A., Phys. Rev., 58, 371 (1940).

22. Read, T. A., Trans. AIME, 143, 30 (1941).

23. Koehler, J. S., Imperfection in Nearly Perfect Crystals, Wiley, New York, 1952, p. 197.

24. Nowick, A. S., Phys. Rev., 80, 259 (1950).

25. Weertman, J., J. Appl. Phys., 26, 202 (1955).

26. Weertman, J., and Salkovitz, E. I., Acta Met., 3, 1 (1955).

27. DeWitt, G., and Koehler, J. S., Phys. Rev., 116, 1113 (1959).

28. Granato, A., and Lücke, K., J. Appl. Phys., 27, 583 (1956).

29. Suzuki, T., Unpublished paper.

30. Fisher, E. S., and Dever, D., Trans. AIME, 239, 48 (1967).

31. Duggin, M. J., and Rachinger, W. A., Acta Met., 12, 1015 (1964).

32. Truell, R., Elbaum, C., and Chick, B. B., Ultrasonic Methods in Solid State Physics, Academic Press, New York and London, 1969, p. 80.

33. McSkimin, H. L., J. Acoust. Soc. Am., 33, 12 (1961).

34. Fowler, A. K., Technical Memorandum No. 2, Panametrics Inc., 1969.

35. Kaufman, L., and Cohen, M., Trans. AIME, 206, 1393 (1956).

36. Becker, R., and Döring, W., Ferromagnetismus, Verlag von Julius Springer, 1939, p. 355.

37. Suzuki, T., and Wuttig, M., "The Triggering Mechanism of the Martensitic Transformation", submitted to Acta Met.

38. Rohde, R. W., and Graham, R. A., Trans. AIME, 245, 2441 (1969).

39. Alers, G. A., Neighbours, J. R., and Sato, H., J. Phys. Chem. Solids, 13, 40 (1960).

40. Jana, S., and Wayman, C. M., Trans. AIME, 239, 1187 (1967).

41. Wuttig, M., Unpublished data.

42. McReynolds, A. W., J. Appl. Phys., 20, 896 (1949).

43. Vogt, E., Magnetic Moments and Transition Temperature in Magnetism and Metallurgy, vol. 1, Academic Press, New York and London, 1969, p. 314.

VII. VITA

Chung Lim was born on February 16, 1942, in Chunju, Korea. He has received his primary and high school education in Chunju, Korea. He received a Bachelor of Science Degree in Metallurgical Engineering from Seoul National University, in Seoul, Korea, in February 1964. After serving in Korean Army as an Ordnance Officer for two years, he was employed by Inchon Ironworks Company, Inchon, Korea, and attained the position of Senior Engineer in charge of electric iron-melting furnace before leaving in June 1969.

He has been enrolled in the Graduate School of the University of Missouri-Rolla since September 1969 and has been appointed as a Graduate Research Assistant since February 1970.

APPENDIX I

EQUATION OF MOTION FOR THE VIBRATING DISLOCATION MODEL

A. BASIC ASSUMPTION

(1) In the absence of the applied stress, only small displacements from the equilibrium position are considered.

(2) Change in potential energy of a dislocation due to bowing out is given by

$$U = C(l - l_o) \tag{AI-1}$$

where l_o is the distance between pinning points, l is the length of a bowed-out dislocation, and C is the line tension of the dislocation.

(3) l_o is the same for all dislocation segments.

(4) The interactions between different dislocation segments are neglected.

(5) Unpinning is not considered.

B. FORMULATION OF THE EQUATIONS

The strain ε is composed of two kinds, the elastic strain ε_{el} and a dislocation strain ε_d, i.e.,

$$\varepsilon = \varepsilon_{el} + \varepsilon_d \tag{AI-2}$$

The elastic strain is given by elasticity theory:

$$\varepsilon_{el} = \sigma/G \tag{AI-3}$$

The dislocation strain ε_d of a dislocation length l_o is given by

$$\varepsilon_d = \frac{N\,b}{l_o} \int_o^{l_o} X(y)\, dy \tag{AI-4}$$

where N is the density of dislocations in the solid, b is the magnitude of the Burgers vector, y is coordinate along the dislocation line, and X is the displacement of a dislocation.

The Newton's equation for the strain ε in the direction of z is

$$\rho \frac{\partial^2 \varepsilon}{\partial t^2} = \frac{\partial^2 \sigma}{\partial z^2} \tag{AI-5}$$

Therefore, Eq. (AI-5) becomes

$$\frac{\partial^2 \sigma}{\partial z^2} - \frac{\rho}{G} \frac{\partial^2 \sigma}{\partial t^2} = \frac{N\rho b}{l_o} \frac{\partial^2}{\partial t^2} \int_o^{l_o} X(y)\, dy \tag{AI-6}$$

The length l of a bowed-out dislocation is given by

$$\begin{aligned} l &= \int_o^{l_o} \left[1 + \left(\frac{dX}{dy}\right)^2\right]^{\frac{1}{2}} dy \\ &= \int_o^{l_o} \left[1 + \frac{1}{2}\left(\frac{dX}{dy}\right)^2 - \frac{1}{8}\left(\frac{dX}{dy}\right)^4 + - - -\right] dy \end{aligned} \tag{AI-7}$$

Therefore, the change in potential energy U is given by

$$U = C \int_o^{l_o} \left[\frac{1}{2}\left(\frac{dX}{dy}\right)^2 - \frac{1}{8}\left(\frac{dX}{dy}\right)^4 + - - -\right] dy \tag{AI-8}$$

The kinetic energy of the dislocation is given by

$$T = \frac{A}{2} \int_o^{l_o} \left(\frac{dX}{dt}\right)^2 dy \tag{AI-9}$$

where A is the effective mass of the dislocation per unit length given by $\pi\rho b^2$. The transformation of the displacement of the dislocation into normal coordinates is achieved through

$$X = \sum_{n=0}^{\infty} Xn \frac{4}{(2n+1)\pi} \sin \frac{(2n+1)}{l_o} \pi y \qquad \text{(AI-10)}$$

Inserting Eq. (AI-10) into Eq. (AI-8) and Eq. (AI-9) and performing the integration, we obtain

$$U = \frac{16}{\pi^2} C \left(\frac{l_o}{4} \Sigma_n X_n^2 \frac{\pi^2}{l_o^2} - \frac{16}{\pi^2} \frac{l_o}{8} \frac{3}{8} \Sigma_n X_n^4 \frac{\pi^4}{l_o^4} + - - - \right) \qquad \text{(AI-11)}$$

$$T = \frac{16}{\pi^2} \frac{A}{2} \Sigma_n \dot{X}_n^2 \frac{1}{(2n+1)^2} \frac{l_o}{2} \qquad \text{(AI-12)}$$

Taking into account the effects of the dissipative force and externally applied stress, the equation of motion for one of the normal coordinates X_n is given by

$$\frac{d}{dt}\left(\frac{\partial L}{\partial \dot{X}_n}\right) - \left(\frac{\partial L}{\partial X_n}\right) + B_n \int_o^{l_o} \left(\frac{\partial X}{\partial t}\right) dy = b\sigma \int_o^{l_o} \left(\frac{\partial X}{\partial X_n}\right) dy \qquad \text{(AI-13)}$$

where $L = T-U$, the Lagrangian and B_n, the damping coefficient per unit length.

Inserting Eqs. (AI-11) and (AI-12) into Eq. (AI-13), we obtain

$$\frac{8}{\pi^2}\,\frac{A\,l_o}{(2n+1)^2}\,\frac{\partial^2 X_n}{\partial t^2} + \frac{8X_n}{\pi^2} C\,l_o\,\frac{\pi^2}{l_o^2} - \frac{8}{\pi^2} C\,l_o\,\frac{16}{\pi^2}\,\frac{3}{8}$$

$$\frac{\pi^4}{l_o^4} X_n^3 + - - - + B_n\,\frac{8\,l_o}{(2n+1)^2\pi^2}\,\frac{\partial X_n}{\partial t} =$$

$$\frac{8\,l_o}{(2n+1)^2\pi^2}\; b\sigma$$

or

$$A\,\frac{\partial^2 X_n}{\partial t^2} + B\,\frac{\partial X_n}{\partial t} + \frac{\pi^2}{l_o^2}\,(2n+1)^2 X_n - C\,\frac{6\pi^2}{l_o^4}\,(2n+1)^2$$

$$X_n^3 + - - - \;= b\sigma \qquad \text{(AI-14)}$$

The equation of motion for the first coordinate is thus given by

$$A\,\frac{\partial^2 X_o}{\partial t^2} + B\,\frac{\partial X_o}{\partial t} + C\,\frac{\pi^2}{l_o^2} X_o - C\frac{6\pi^2}{l_o^4} X_o^3 + - - = b\sigma \qquad \text{(AI-15)}$$

APPENDIX II

ATTENUATION AND VELOCITY CHANGE OF ULTRASONIC WAVE

Consider a differential equation for the vibrating dislocation model as in the Appendix I.

$$A \frac{\partial X}{\partial t^2} + B \frac{\partial X}{\partial t} + PX = b\sigma \tag{AII-1}$$

The applied stress may be represented by

$$\sigma = \sigma_o \, e^{-\alpha z} \, e^{i(\omega t - kz)} \tag{AII-2}$$

$$X = \sum_n X_n \frac{4}{(2n + 1)\pi} \sin \left(\frac{2n + 1}{l_o} \right) \pi y \tag{AII-3}$$

where X_n is one of the solutions of Eq. (AII-1). Let

$$X_n = K_n \, e^{i(\omega t - \delta_n)} \tag{AII-4}$$

Inserting Eq. (AII-4) into Eq. (AII-1), we have

$$K_n [A(-\omega^2) + Bi\omega + P] e^{i(\omega t - \delta_n)} = b\sigma_o e^{-\alpha z} e^{i(\omega t - kz)}$$

Thus

$$K_n = \frac{b\sigma_o \, e^{-\alpha z} e^{-ikz}}{[(P - A\omega^2)^2 + (B\omega)^2]^{\frac{1}{2}}} \tag{AII-5}$$

and

$$\left.\begin{aligned}
\cos \delta_n &= \frac{P - A\omega^2}{[(P - A\omega^2)^2 + (B\omega)^2]^{\frac{1}{2}}} \\
\sin \delta_n &= \frac{B\omega}{[(P - A\omega^2)^2 + (B\omega)^2]^{\frac{1}{2}}} \\
\tan \delta_n &= \frac{B\omega}{P - A\omega^2}
\end{aligned}\right\} \qquad \text{(AII-6)}$$

From Eqs. (AII-3), (AII-4) and (AII-5) we obtain

$$X_n = \frac{b\sigma_o e^{-\alpha z} e^{-ikz}}{[(P - A\omega^2)^2 + (B\omega)^2]^{\frac{1}{2}}} e^{i(\omega t - \delta_n)} \qquad \text{(AII-7)}$$

and therefore

$$X = \frac{4}{\pi} b\sigma_o e^{-\alpha z} e^{i(\omega t - kz)} \Sigma \frac{1}{(2n+1)} \sin \left(\frac{2n+1}{l_o}\right)\pi y \cdot$$

$$\frac{e^{-i\delta_n}}{[(P - A\omega^2)^2 + (B\omega)^2]^{\frac{1}{2}}} = \frac{4b\sigma}{\pi} \sum_n \frac{1}{(2n+1)} \sin \left(\frac{2n+1}{l_o}\right)\pi y \cdot$$

$$\frac{e^{-i\delta_n}}{[(P - A\omega^2)^2 + (B\omega)^2]^{\frac{1}{2}}} \qquad \text{(AII-8)}$$

Now inserting Eqs. (AII-8) and (AII-2) into Eq. (AI-6) given in Appendix I, which is

$$\frac{\partial^2 \sigma}{\partial z^2} - \frac{\rho}{G} \frac{\partial^2 \sigma}{\partial t^2} = \frac{N\rho b}{l_o} \frac{\partial^2}{\partial t^2} \int_o^{l_o} X(y)\, dy \qquad \text{(AII-9)}$$

we have

$$\sigma_o(\alpha + ik)^2 e^{-\alpha z} e^{i(\omega t - kz)} - \frac{\rho}{G} \sigma_o(-\omega^2) e^{-\alpha z} e^{i(\omega t - kz)}$$

$$= \frac{N\rho b}{l_o} \frac{\partial^2}{\partial t^2} \left[\frac{4b\sigma}{\pi} \sum_n \frac{1}{(2n+1)} \int_o^{l_o} \sin \left(\frac{2n+1}{l_o} \right) \pi y \cdot \frac{e^{i\delta_n}}{[(P - A\omega^2)^2 + (B\omega)^2]^{\frac{1}{2}}} dy \right]$$

$$= \frac{N\rho b}{l_o} (-\omega^2) \frac{4b\sigma}{\pi} \sum_n \frac{2 l_o}{(2n+1)^2 \pi} \frac{e^{-i\delta_n}}{[(P - A\omega^2)^2 + (B\omega)^2]^{\frac{1}{2}}} \qquad \text{(AII-10)}$$

For the first normal coordinate, i.e., for n=0

$$(\alpha^2 - k^2 + 2i\alpha k) + \frac{\rho}{G} \omega^2$$

$$= - \frac{8N\rho b^2}{\pi^2} \omega^2 \frac{(\cos \delta_n - i \sin \delta_n)}{[(P - A\omega^2)^2 - (B\omega)^2]^{\frac{1}{2}}} \qquad \text{(AII-11)}$$

Equating separately the real part and the imaginary part of the both sides, we get

$$2i\alpha k = \frac{8N\rho b^2}{\pi^2} \omega^2 \frac{-(-i \sin \delta_o)}{[(P - A\omega^2)^2 + (B\omega)^2]^{\frac{1}{2}}} \qquad \text{(AII-12)}$$

$$(\alpha^2 - k^2) + \frac{\rho}{G} \omega^2 = - \frac{8N\rho b^2}{\pi^2} \omega^2 \frac{\cos \delta_o}{[(P - A\omega^2)^2 + (B\omega)^2]^{\frac{1}{2}}} \qquad \text{(AII-13)}$$

Inserting the values of $\cos \delta_o$ and $\sin \delta_o$ given by Eq. (AII-6) into these Eqs., we have

$$\alpha = \frac{\omega^2}{2k} \cdot \frac{8N\rho b^2}{\pi^2} \cdot \frac{B\omega}{[(P - A\omega^2)^2 + (B\omega)^2]}$$

$$= \frac{4NGb^2}{V\pi^2} \cdot \frac{B\omega^2}{[(P - A\omega^2)^2 + (B\omega)^2]}$$

$$= \frac{4NGb^2}{AV\pi^2} \cdot \frac{\omega^2 d}{(\omega_o^2 - \omega^2)^2 + (\omega d)^2} \qquad \text{(AII-14)}$$

where $V = (G/\rho)^{\frac{1}{2}} = (\omega/k)$: velocity of the ultrasonic wave

ω: angular frequency

$\omega_o = (P/A)^{\frac{1}{2}}$: angular resonance frequency of the dislocation line

$d = B/A$

and also

$$(\alpha^2-k^2) + \frac{\rho}{G}\omega^2 = -\frac{8N\rho b^2}{\pi^2}\omega^2 \cdot \frac{(P-A\omega^2)}{[(P-A\omega^2)^2+(B\omega)^2]} . \quad \text{(AII-15)}$$

Since $\alpha << k$, we can neglect the α^2 term in Eq. (AII-15). It follows that

$$\frac{\omega^2}{k^2} = \frac{G}{\rho}\left(1 - \frac{\omega^2}{k^2}\frac{8N\rho b^2}{\pi^2} \cdot \frac{(P-A\omega^2)}{[(P-A\omega^2)^2+(B\omega)^2]}\right)$$

or

$$\frac{\omega}{k} = \left(\frac{G}{\rho}\right)^{\frac{1}{2}}\left(1 - \frac{1}{2}\frac{8NGb^2}{\pi^2} \cdot \frac{(P-A\omega^2)}{[(P-A\omega^2)^2+(B\omega)^2]}\right) \quad \text{(AII-16)}$$

where 3rd and higher order terms in the binomial expansion are neglected. Therefore,

$$V_T(\omega) = V\left(1 - \frac{4NGb^2}{A\pi^2} \cdot \frac{(\omega_o^2 - \omega^2)}{[(\omega_o^2 - \omega^2)^2+(\omega d)^2]}\right) \quad \text{(AII-17)}$$

and the relative change of the velocity $\Delta V/V$ is given by

$$\frac{V_T - V}{V} = \frac{\Delta V}{V} = -\frac{4NGb^2}{A\pi^2} \cdot \frac{\omega_o^2 - \omega^2}{(\omega_o^2 - \omega^2)^2+(\omega d)^2} \quad \text{(AII-18)}$$

Appendices I and II are based on the papers

1) Granato, A. and Lücke, K., J. Appl. Phys., 27, p. 583, (1956).

2) Suzuki, T., Hikata, A., and Elbaum, C., J. Appl. Phys., 27, p. 2761, (1964).